



จุฬาลงกรณ์มหาวิทยาลัย
ทุนวิจัย
กองทุนรัชดาภิเษกสมโภช

รายงานวิจัย

การศึกษาทางทฤษฎีของการถ่ายโอนอิเล็กทรอนิกส์จากการเหนี่ยวนำแสง
ในโปรตีนเอฟเอ็มเอ็น:อิทธิพลจากการเปลี่ยนประจุ
ของกรดอะมิโนที่มีผลต่ออัตราการถ่ายโอนอิเล็กทรอนิกส์

โดย

สมศักดิ์ เพ็ชรวิช
ศิริรัตน์ กักผล

กรกฎาคม 2556

กิตติกรรมประกาศ

ผู้วิจัยขอขอบพระคุณกองทุนรัชดาภิเษกสมโภช จุฬาลงกรณ์มหาวิทยาลัย ที่ให้ทุนสนับสนุนการทำวิจัย และหน่วยปฏิบัติการวิจัยเคมีคอมพิวเตอร์ ภาควิชาเคมี คณะวิทยาศาสตร์ จุฬาลงกรณ์มหาวิทยาลัย สำหรับทรัพยากรคอมพิวเตอร์ต่าง ๆ

ชื่อโครงการวิจัย การศึกษาทางทฤษฎีของการถ่ายโอนอิเล็กทรอนิกส์จากการเหนี่ยวนำแสงในโปรตีนเอฟเอ็ม
เอิน: อิทธิพลจากการเปลี่ยนประจุของกรดอะมิโนที่มีผลต่ออัตราการถ่ายโอนอิเล็กทรอนิกส์

ชื่อผู้วิจัย ผศ.ดร. สมศักดิ์ เพ็ญรวณิช และ รศ.ดร. ศิริรัตน์ กักผล

เดือนและปีที่ทำวิจัยเสร็จ เมษายน 2555

บทคัดย่อ

การถ่ายโอนอิเล็กทรอนิกส์ที่เหนี่ยวนำด้วยแสง (พีอีที) เป็นกระบวนการที่มีความสำคัญเพราะสามารถนำไปประยุกต์ใช้ได้หลายด้าน เช่น การเปลี่ยนแสงเป็นพลังงาน พลาโวโปรตีนมักถูกเลือกมาใช้เป็นแบบจำลองสำหรับการศึกษาพีอีที ในงานวิจัยนี้ทำการศึกษาอิทธิพลของประจุที่เรลิติว 13 ที่มีต่อพีอีทีจากกรดอะมิโนทริปโตเฟน 32, ไทโรซีน 35 และทริปโตเฟน 106 ไปยังไอโซอัลลอกซาซินที่ถูกกระตุ้นในโปรตีนที่จับกับเอฟเอที (เอฟบีพี) ที่แยกมาจากแบคทีเรียดีซัลโฟวิบริโอ วัลการิส (มียาซากิ เอ็ฟ) โดยทำการคำนวณโมเลกุลาร์ไดนามิกซิมูเลชัน (เอ็มดี) ของระบบเอฟบีพีชนิดดั้งเดิม (อี 13 ที่มีประจุเป็นลบ) และชนิดกลายพันธุ์ที่ตำแหน่ง 13 จำนวน 4 ชนิด คือ อี 13 เค และ อี 13 อาร์ (ประจุบวก), อี 13 ที และ อี 13 คิว (ประจุเป็นกลาง) จากนั้นนำโครงสร้างที่เวลาต่าง ๆ ที่ได้จากการคำนวณเอ็มดีมาใช้ในการหาค่าอัตราเร็วพีอีทีด้วยทฤษฎีคาติทานิและมาทาเกะ ผลการวิจัยพบว่าอัตราเร็วพีอีทีขึ้นอยู่กับพลังงานไฟฟ้าสถิตระหว่างผลิตภัณฑ์แสงและกลุ่มไอออนต่าง ๆ แต่ไม่ขึ้นกับค่าทางกายภาพอื่น ๆ ที่เกี่ยวข้องกับอัตราเร็วพีอีที เช่น พลังงานการจัดตัวใหม่ตามตัวทำละลาย กราฟระหว่างอัตราเร็วพีอีทีกับค่าช่องว่างพลังงานเสรีรวมมีลักษณะเป็นฟังก์ชันพาราโบลา และกราฟระหว่างอัตราเร็วพีอีทีกับพลังงานไฟฟ้าสถิตระหว่างผลิตภัณฑ์แสงและกลุ่มไอออนต่าง ๆ มีลักษณะเป็นฟังก์ชันพาราโบลาเช่นกัน ผลเหล่านี้แสดงว่าพลังงานไฟฟ้าสถิตสุทธิมีอิทธิพลเป็นอย่างมากต่ออัตราเร็วพีอีที นอกเหนือไปจากระยะห่างระหว่างตัวให้กับตัวรับ

จพ

เลขหมู่ 2 15

เลขทะเบียน 016736

วัน, เดือน, ปี 21ก.ค. 58

Project Title Theoretical Analysis of Photoinduced Electron Transfer in FMN Binding Protein:
Effect of Changes in One Charge on Electron Transfer Rate

Name of the Investigators Somsak Pianwanit and Sirirat Kokpol

Year April 2012

Abstract

Photoinduced electron transfer (PET) is an important process due to its several applications, e.g. solar energy conversion. Flavoproteins are generally selected as a model for the study of PET. In this research, effect of charge at residue 13 on the PET from Trp32, Tyr35 and Trp106 to an excited isoalloxazine (Iso*) in FMN binding protein (FBP) from *Desulfovibrio vulgaris* (Miyazaki F) was studied. A wild type (E13 with negative charge) and four mutations of FBP at residue 13, E13K and E13R (positive charge), E13T and E13Q (neutral charge), were subjected to molecular dynamics (MD) simulations. Snap shots obtained from the MD simulations were used to evaluate the PET rate using the Kakitani and Mataga theory. The PET rates were found to largely depend on the electrostatic energies between photo-products and other ionic groups but not on other physical quantities related to the PET rate such as solvent reorganization energies. A plot of the PET rates vs. total free energy gaps displayed a parabolic function. Similarly, the plot of the PET rates vs. the net electrostatic energies between photo-products and other ionic groups also displayed a parabolic function. This reveals that the net electrostatic energies are most influential upon the ET rate, in addition to the donor-acceptor distance.

สารบัญ

	หน้า
กิตติกรรมประกาศ	i
บทคัดย่อภาษาไทย	ii
บทคัดย่อภาษาอังกฤษ	iii
บทความตีพิมพ์ใน <i>Phys. Chem. Chem. Phys.</i> , 2011, 13, 6085-6097.	1
ร่างบทความส่งไปพิจารณาที่ <i>J. Phys. Chem.</i>	15

งานวิจัยตามโครงการวิจัยนี้ มีผลการวิจัยที่ได้รับการตีพิมพ์แล้วจำนวน 1 บทความ และอยู่ในระหว่างการพิจารณาของวารสารทางวิชาการอีก 1 บทความ ดังนั้นเนื้อหาทั้งหมด (บทนำ วิธีการวิจัย ผลการวิจัย การอภิปรายผล และข้อสรุป) จึงอยู่ในบทความทั้งสองนี้ และได้ทำการแนบเอกสารดังกล่าวมาในรายงานฉบับนี้ คือ

1. Nadtanet Nunthaboot, Somsak Pianwanit, Sirirat Kokpol, Fumio Tanaka, Simultaneous analyses of photoinduced electron transfer in the wild type and four single substitution isomers of the FMN binding protein from *Desulfovibrio vulgaris*, Miyazaki F, *Phys. Chem. Chem. Phys.*, 2011, **13**, 6085-6097. (Impact Factor ปี 2010 = 3.454)
2. Nadtanet Nunthaboot, Kiattisak Lugsanangarm, Arthit Nueangaudom, Somsak Pianwanit, Sirirat Kokpol, Fumio Tanaka, Role of the Electrostatic Energy between the Photo-Products and Ionic Groups on the Photoinduced Electron Transfer from Aromatic Amino Acids to the Excited Flavins in Five FMN Binding Proteins. Effects of Negative, Positives and Neutral Amino Acids on the Rates, submitted to *The Journal of Physical Chemistry*.

Cite this: *Phys. Chem. Chem. Phys.*, 2011, 13, 6085–6097

www.rsc.org/pccp

PAPER

Simultaneous analyses of photoinduced electron transfer in the wild type and four single substitution isomers of the FMN binding protein from *Desulfovibrio vulgaris*, Miyazaki F†

Nadtanet Nunthaboot,^a Somsak Pianwanit,^{*b} Sirirat Kokpol^b and Fumio Tanaka^{*c}

Received 23rd November 2010, Accepted 17th January 2011

DOI: 10.1039/c0cp02634d

The mechanism of photoinduced electron transfer (PET) from the aromatic amino acids (Trp32, Tyr35 and Trp106) to the excited flavin mononucleotide (FMN) in the wild type (WT) and four single amino acid substitution isomers (E13T, E13Q, W32A and W32Y) of FMN binding protein (FBP) from the *Desulfovibrio vulgaris* (Miyazaki F) were simultaneously analyzed (Method A) with the Marcus–Hush (MH) theory and Kakitani–Mataga (KM) theory using ultrafast fluorescence dynamics of these proteins. In addition, the PET mechanism of the WT, E13T and E13Q FBP systems (Method B) were also analyzed with both MH and KM theories. The KM theory could describe all of the experimental fluorescence decays better than the MH theory by both Methods A and B. The PET rates were found to largely depend on the electrostatic energies between photo-products, isoalloxazine (Iso) anion and the PET donor cations, and the other ionic groups, and hence on static dielectric constants. The dielectric constant (ϵ_0^{DA}) around the PET donors and acceptor was separately determined from those (ϵ_0^j , $j = \text{WT, E13T, E13Q, W32Y}$ and W32A) in the domain between the Iso anion or the donor cations and the other ionic groups in the proteins. The values of ϵ_0^{DA} were always lower than those of ϵ_0^j , which is reasonable because no amino acid exists between the PET donors and acceptor in all systems. The values of the dielectric constants ϵ_0^j ($j = \text{WT, E13T}$ and E13Q) were similar to those obtained previously from the analysis of the crystal structures and the average lifetimes of these FBP proteins. Energy gap law in the FBP systems was examined. An excellent parabolic function of the logarithms of the PET rates was obtained against the total free energy gap. The PET in these FBP isomers mostly took place in the so-called normal region, and partly in the inverted region.

1. Introduction

Electron transfer phenomena have been important subjects in the fields of physics, chemistry and biology.^{1,2} The photo-induced electron transfer (PET) plays an essential role in photosynthetic systems.³ In the last decade a number of new flavin photoreceptors have been found,⁴ including the BLUF (blue-light using flavin) units of the flavin photoreceptors that contain Tyr and/or Trp near isoalloxazine (Iso). The PET from Tyr to the excited Iso (Iso*) is considered to be the first step of the photo-regulation for photosynthesis in AppA⁵ and

pili-dependent cell motility in TePixD⁶ and Slr1694⁶ in the BLUF-containing photoactive bacteria.

Fluorescence quenching of flavins by various substances, including aromatic amino acids, was first investigated by Weber.⁷ McCormick demonstrated a remarkable quenching of fluorescence from Iso* by Trp in series of compounds in which Iso and Trp are covalently linked.⁸ Time-resolved fluorescence of flavins and flavoproteins has been reviewed by van den Berg and Visser.⁹ Most of the flavoproteins, other than the flavin photoreceptors, contain the aromatic amino acids Trp and Tyr near the Iso and these flavoproteins are practically non-fluorescent. However, they emit fluorescence with very short lifetimes following excitation with a sub-picosecond light pulse.^{10–15} This remarkable fluorescence quenching is considered to be ascribed to the ultrafast PET in these flavoproteins from the Trp and/or Tyr to the Iso*.^{16–19}

Since the seminal works on electron transfer theory by Marcus,²⁰ several researchers have further developed the PET theory.^{21,22} However, these have been modeled for PET

^a Department of Chemistry, Faculty of Science, Mahasarakham University, Mahasarakham, 44150, Thailand

^b Department of Chemistry, Faculty of Science, Chulalongkorn University, Bangkok, 10330, Thailand. E-mail: somsak.t@chula.ac.th

^c Department of Biochemistry, Center for Excellence in Protein Structure and Function, Faculty of Science, Mahidol University, Bangkok, 10400, Thailand. E-mail: fukoh2003@yahoo.com

† Electronic supplementary information (ESI) available. See DOI: 10.1039/c0cp02634d

in bulk solution and it is not clear whether these theories are applicable to PET in proteins. To this end it is required to establish a method to quantitatively analyze PET in proteins. The PET rates in flavoproteins have been analyzed with ultrafast fluorescence dynamics and Kakitani and Mataga (KM) theory using the atomic coordinates obtained by molecular dynamics simulation (MD).^{23–26} The procedure to determine the unknown PET parameters was performed as follows: (1) the time-dependent atomic coordinates of flavoproteins were obtained by MD, (2) the PET rates were calculated using a PET theory and the atomic coordinates with a set of trial PET parameters, (3) the parameters were varied until the best-fit between the calculated and observed fluorescence decays was obtained, according to a non-linear least squares method.

Recently, it has been demonstrated that disappearance of only one negative charge in the wild type (WT) flavin mononucleotide (FMN) binding proteins (FBP) modifies the ultrafast fluorescence dynamics, and consequentially the PET rates in E13T and E13Q.²⁷ This suggests that electrostatic interactions between ionic photoproducts and the other ionic groups in the proteins are the most influential factors upon the PET rate from Trp and/or Tyr to Iso*, together with the donor–acceptor distances. Static (averaged) lifetimes of the WT FBP, and the single substitution E13T and E13Q isomers, have been analyzed from their X-ray structures. It is important to obtain common PET parameters in FBP protein systems, because some of them can be used for electron transfer processes in FBP without light. In the present work, we have simultaneously analyzed the ultrafast fluorescence dynamics of the WT and four single substitution isoforms (E13T, E13Q, W32Y and W32A) of FBPs with Marcus and Hush (MH) theory²⁰ and KM theory,²² to determine the common PET parameters, and also to establish the method of the PET analysis. The effect of the disappearance of the negative charge in the WT FBP at Glu13 on the PET rate was also examined with ultrafast fluorescence dynamics of these systems and the protein structures obtained by MD.

II. Methods of analyses

MD calculation

The starting structures of the WT and its mutated FBPs were obtained by using the X-ray structure of the *D. vulgaris* (Miyazaki F) WT FBP (PDB code 1FLM).²⁸ In the E13T and E13Q single substitution isomers, the glutamate at position 13 was replaced by threonine and glutamine, respectively, and the replacement of amino acids from the WT was conducted using the LEap module implemented in AMBER 8.²⁹ All calculations were carried out using the AMBER 8 suite of programs. The parm99 force field³⁰ was used to describe the protein atoms whereas force field parameters for Iso were obtained from Schneider and Suhnel.³¹ All missing hydrogen atoms of the protein were added using the LEap module of AMBER 8. The simulated systems were subsequently solvated with a cubic box of 6336 TIP3P water molecules. This is almost comparable to that of 6345 and 6347 in the case of W32Y and W32A, respectively.²⁴

The electroneutrality of the systems was attained by adding 1 chloride counterion. The added water molecules were first minimized, while the protein and Iso coordinates were kept fixed. The entire system was then optimized using 2000 steps of steepest descent and conjugated gradient minimizations. Afterwards, the whole system was heated from 10 K to 298 K over 50 ps and was further equilibrated under periodic boundary conditions at 298 K. The systems were set up under the isobaric–isothermal ensemble (NPT) with a constant pressure of 1 atm and constant temperature of 298 K. Electrostatic interaction was corrected by the Particle Mesh Ewald method.³² The SHAKE algorithm³³ was employed to constrain all bonds involving hydrogen atoms. A cutoff distance of 1 nm was employed for non-bonded pair interactions. MD based calculations were performed with the time steps of 2 fs and the coordinates of the MD snapshots were collected every 0.01 ps. The simulations were performed over 5 ns. Data collected during the last 3 ns were used to analyze and to compare with that from previous MDs of W32Y and W32A FBP systems.²⁴

PET theory

MH,²⁰ Bixon and Jortner (BJ),²¹ and KM theories²² were applied for the PET process in the WT FBP.²³ The observed fluorescence decay was satisfactorily reproduced with MH and KM theories. However, only the decay of the WT FBP was examined by these PET theories. In the present work, we have simultaneously examined five decays of WT, E13T, E13Q, W32Y and W32A FBP systems with both MH and KM theories.

The PET rate from a donor k to Iso* in the j th FBP system given by MH theory (k_{MH}^j) is expressed as eqn (1).²⁰

$$k_{\text{MH}}^j = \frac{2\pi}{\hbar} \frac{H_q^2}{\sqrt{4\pi\lambda_S^j k_B T}} \times \exp \left[-\frac{\left\{ \Delta G_q^0 - e^2/\epsilon_0^{\text{DA}} R_{jk} + \lambda_S^j + ES_j(k) \right\}^2}{4\lambda_S^j k_B T} \right] \quad (1)$$

where H_q is the electronic interaction energy between Iso* and the donor q (Trp or Tyr), assuming that H_q depends only on q , and not on j and k . R_{jk} is the center-to-center distance between Iso and the PET donor k in the j th FBP system. For this FBP, $j = 1, 2, 3, 4$, and 5 for the WT, E13T, E13Q, W32Y and W32A isoforms, respectively, whilst $k = 0$ for Iso, $k = 1$ for Trp32 (Tyr32 in W32Y), $k = 2$ for Tyr35 and $k = 3$ for Trp106. The PET rate may be dependent on both j and k . \hbar , k_B , T and e are the reduced Planck's constant, Boltzmann's constant, temperature (298 K) and electron charge, respectively. ϵ_0^{DA} is a static dielectric constant of medium between PET donors and acceptor. $ES_j(k)$ is a net electrostatic (ES) energy between the k th aromatic ionic species and all the other ionic groups in the j th FBP system, as described below. λ_S^j is the solvent reorganization energy of the Iso* and the k th donor in the j th FBP system, as shown by eqn (2).

$$\lambda_S^j = e^2 \left(\frac{1}{2a_{\text{Iso}}} + \frac{1}{2a_q} - \frac{1}{R_{jk}} \right) \left(\frac{1}{\epsilon_\infty} - \frac{1}{\epsilon_0^{\text{DA}}} \right) \quad (2)$$

Here, a_{Iso} and a_q are the radii of Iso and the donor q (Trp or Tyr), assuming these reactants are spherical, and ϵ_∞ is optical dielectric constant (a value of 2 being used). The radii of Iso, Trp and Tyr were determined as previously reported,^{23–26} with values of $a_{\text{Iso}} = 0.224$ nm, and $a_{\text{Trp}} = 0.196$ nm and $a_{\text{Tyr}} = 0.173$ nm being used.

The standard free energy gap (ΔG_q^0) was expressed with the ionization potential (E_{IP}^q) of the PET donor q (Trp or Tyr), as eqn (3).

$$\Delta G_q^0 = E_{\text{IP}}^q - G_{\text{Iso}}^0 \quad (3)$$

where G_{Iso}^0 is the standard Gibbs energy related to the electron affinity of Iso*. The values of E_{IP}^q for Trp and Tyr were 7.2 eV and 8.0 eV, respectively.³⁴

The PET rate from the donor k to Iso* in the j th FBP system, as given by the KM theory (k_{KM}^{jk}), is expressed as eqn (4).²²

$$k_{\text{KM}}^{jk} = \frac{\nu_0^q}{1 + \exp\{\beta^q(R_{jk} - R_0^q)\}} \sqrt{\frac{k_{\text{B}}T}{4\pi\lambda_S^{jk}}} \times \exp\left[-\frac{\left\{\Delta G_q^0 - e^2/\epsilon_0^{\text{DA}}R_{jk} + \lambda_S^{jk} + ES_j(k)\right\}^2}{4\lambda_S^{jk}k_{\text{B}}T}\right] \quad (4)$$

Here ν_0^q is an adiabatic frequency, β^q is the PET process coefficient, and R_0^q is a critical distance between the adiabatic and non-adiabatic PET processes. These quantities depend only on q (Trp or Tyr), and when $R_{jk} < R_0^q$ the PET process may be adiabatic, whereas when $R_{jk} > R_0^q$ the PET process is non-adiabatic. The meanings of all the other quantities are the same as those in MH theory.

ES energy in the proteins

Proteins, including the FBPs, contain many ionic groups, which may influence the PET rate. The WT, and the single-substitution E13T and E13Q isoforms of the *D. vulgaris* (Miyazaki F) FBP contain Trp32, Tyr35 and Trp106 as potential PET donors, whilst W32Y contains Tyr32, Tyr35 and Trp106 as PET donors and W32A contains only Tyr35 and Trp106. The cofactor in all these FBP systems is FMN, which has two negative charges at the phosphate. The WT, W32Y and W32A isoforms contain 8 Glu, 5 Asp, 4 Lys and 9 Arg residues, whereas E13T and E13Q have 7 Glu residues since the Glu13 was replaced by the neutral Thr13 and Gln13, respectively. The ES energy between the Iso anion or donor k cation, and all the other ionic groups in the FBP system j is expressed by eqn (5):

$$E_j(k) = \sum_{i=1}^n \frac{C_k C_{\text{Glu}}}{\epsilon_0^j R_k(\text{Glu} - i)} + \sum_{i=1}^5 \frac{C_k C_{\text{Asp}}}{\epsilon_0^j R_k(\text{Asp} - i)} + \sum_{i=1}^4 \frac{C_j C_{\text{Lys}}}{\epsilon_0^j R_k(\text{Lys} - i)} + \sum_{i=1}^9 \frac{C_j C_{\text{Arg}}}{\epsilon_0^j R_k(\text{Arg} - i)} + \sum_{i=1}^2 \frac{C_j C_{\text{P}}}{\epsilon_0^j R_k(\text{P} - i)} \quad (5)$$

where $n = 8$ for the WT, W32Y and W32A, and $n = 7$ for the E13T and E13Q isoforms. Here, $k = 0$ for the Iso anion, $k = 1$ for Trp32⁺ (Tyr32⁺ in W32Y), $k = 2$ for Tyr35⁺ and $k = 3$ for Trp106⁺. ϵ_0^j is the static dielectric constant of the j th FBP system. C_k is the charge of the aromatic ionic species k , and is $-e$ for $k = 0$ (Iso anion), $+e$ for $k = 1$ to 3. $C_{\text{Glu}} (= -e)$, $C_{\text{Asp}} (= -e)$, $C_{\text{Lys}} (= +e)$, $C_{\text{Arg}} (= +e)$ and $C_{\text{P}} (= -e)$ are the charges of Glu, Asp, Lys, Arg and phosphate anions, respectively. We assumed that these groups are all in an ionic state in solution. Distances between the aromatic ionic species k and the i th Glu ($i = 1 - 8$ or 7) are denoted as $R_k(\text{Glu} - i)$, those between k and the i th Asp ($i = 1 - 4$) are denoted as $R_k(\text{Asp} - i)$, and so on.

$ES_j(k)$ in eqn (1) was expressed as follows:

$$ES_j(k) = E_j(0) + E_j(k) \quad (6)$$

Here, j varies from 1 to 5 in Method A and 1 to 3 in Method B with k values from 1 to 3 (k th PET donor), as given in eqn (5).

Fluorescence decays. The experimental fluorescence decay functions of the WT, W32Y and W32A FBP isoforms have been reported by Chosrowjan *et al.*,^{14,15} as given by eqn (7)–(9), respectively, whereas those for E13T and E13Q are given by eqn (10) and (11)²⁷ respectively.

$$F_{\text{obs}}^{\text{WT}} = 0.96\exp(-t/0.167) + 0.04\exp(-t/1.5) \quad (7)$$

$$F_{\text{obs}}^{\text{W32Y}} = 0.23\exp(-t/3.4) + 0.74\exp(-t/18.2) + 0.03\exp(-t/96) \quad (8)$$

$$F_{\text{obs}}^{\text{W32A}} = \exp(-t/30.1) \quad (9)$$

$$F_{\text{obs}}^{\text{E13T}} = 0.86\exp(-t/0.107) + 0.12\exp(-t/1.5) + 0.02\exp(-t/30) \quad (10)$$

$$F_{\text{obs}}^{\text{E13Q}} = 0.85\exp(-t/0.134) + 0.12\exp(-t/0.746) + 0.03\exp(-t/30) \quad (11)$$

The lifetimes are indicated in units of ps. The calculated decay function of the j th FBP system with MH theory is expressed by eqn (12).

$$F_{\text{calc}}^j(t) = \left\langle \exp\left[-\left\{\sum_{k=1}^3 k_{\text{MH}}^k(t')\right\}t\right] \right\rangle_{\text{AV}} \quad (12)$$

The calculated decay function of the j th FBP system with KM theory is expressed by eqn (13):

$$F_{\text{calc}}^j(t) = \left\langle \exp\left[-\left\{\sum_{k=1}^3 k_{\text{KM}}^k(t')\right\}t\right] \right\rangle_{\text{AV}} \quad (13)$$

The fluorescence decays of the WT, E13T and E13Q FBP isoforms were calculated up to 3 ps with 0.003 ps time intervals, whilst that for the W32Y and W32A isoforms were calculated up to 20 ps with 0.02 ps intervals. Note that $\langle \dots \rangle_{\text{AV}}$ denotes the averaging procedure of the exponential function in eqn (12) and (13), and was performed over t' up to 2 ns with 0.1 ps time intervals for the WT, W32Y and W32A isoforms, and up to 3 ns with 0.1 ps intervals for the E13T and E13Q isoforms. In eqn (12) and (13) we assumed that the decay functions at every instant of time (t') during the MD time range can always be expressed by an exponential function. The present method is equivalent to the reported one³⁵ when the

time range ($t' = 2\text{--}3$ ns) of MD data is much longer than that for the fluorescence data (t at most 20 ps). The mathematical basis of the present method is described in ESI† A.

In the MH based analysis, the unknown PET parameters were H_{Trp} , H_{Tyr} , G_{Iso}^0 , ϵ_0^{WT} , ϵ_0^{E13T} , ϵ_0^{E13Q} and ϵ_0^{DA} in Methods A and B, plus ϵ_0^{W32Y} and ϵ_0^{W32A} in Method A. In the KM based analysis the unknown parameters were G_{Iso}^0 , ϵ_0^{WT} , ϵ_0^{E13T} , ϵ_0^{E13Q} and ϵ_0^{DA} in Methods A and B, plus ϵ_0^{W32Y} and ϵ_0^{W32A} in Method A. The previously reported values for t_0^q , β^q and R_0^q ($q = \text{Trp}$ or Tyr) were used.²⁷ To compare the results obtained with crystal structures²⁷ we also analyzed ET parameters by Method B. The chi-squared value of the j th FBP system between the observed and calculated fluorescence intensities (χ_j^2) is defined by eqn (14).

$$\chi_j^2 = \frac{1}{N} \sum_{i=1}^N \frac{\{F_{\text{calc}}^j(t_i) - F_{\text{obs}}^j(t_i)\}^2}{F_{\text{calc}}^j(t_i)} \quad (14)$$

Here, N denotes the number of time intervals of the fluorescence decay, and was 1000 for all evaluations. The deviation between the observed and calculated intensities is expressed by eqn (15).

$$\text{Dev}_j(t_i) = \frac{\{F_{\text{calc}}^j(t_i) - F_{\text{obs}}^j(t_i)\}}{\sqrt{F_{\text{calc}}^j(t_i)}} \quad (15)$$

We determined all of the PET parameters in the MH and KM theories by the two methods:

$$\text{Method A: } \chi_5^2 = \chi_{\text{WT}}^2 + \chi_{\text{E13T}}^2 + \chi_{\text{E13Q}}^2 + \chi_{\text{W32Y}}^2 + \chi_{\text{W32A}}^2 \quad (16)$$

$$\text{Method B: } \chi_3^2 = \chi_{\text{WT}}^2 + \chi_{\text{E13T}}^2 + \chi_{\text{E13Q}}^2 \quad (17)$$

The PET parameters were determined both by MH and KM theories so as to obtain the minimum values of χ_5^2 in Method A and χ_3^2 in Method B, by means of a non-linear least squares method, according to the Marquardt algorithm, as previously reported.^{23–26}

III. Results

Geometrical factors around Iso

The crystal structure of the WT *D. vulgaris* (Miyazaki F) FBP was determined by Suto *et al.*,²⁸ and those of the E13T and E13Q isomers by Nakanishi *et al.*²⁷ The corresponding MD structures of the WT, E13T, E13Q, W32Y and W32A isoforms of FBP are shown in Fig. 1, whilst Fig. 2 shows the time-dependent changes in the center-to-center distances (R_c) between Iso and Trp32, Tyr35 and Trp106 in the WT, E13T and E13Q isoforms, respectively. The distances between Iso and Trp32, between Iso and Tyr35 and between Iso and Trp106 in W32Y and between Iso and Tyr35 and between Iso and Trp106 in W32A, respectively, have already been reported.^{23,24} Here, the WT FBP displayed long term fluctuations in the R_c values, in addition to the instantaneous fluctuation, while such long term fluctuation was not found in the E13T and E13Q isoforms.

The time-dependent changes in the edge-to-edge distances (R_e) between the donors and the Iso are shown in Fig. 3. The R_e fluctuation pattern was somewhat similar to that seen with the R_c values in the WT, E13T and E13Q FBP isoforms. The time-dependent changes in the inter-planar angles between the Iso residue and the indicated PET donor aromatic amino acids are shown in Fig. 4 for the WT, E13T and E13Q isoforms. The variation in the angles was highest in the WT, in accord with

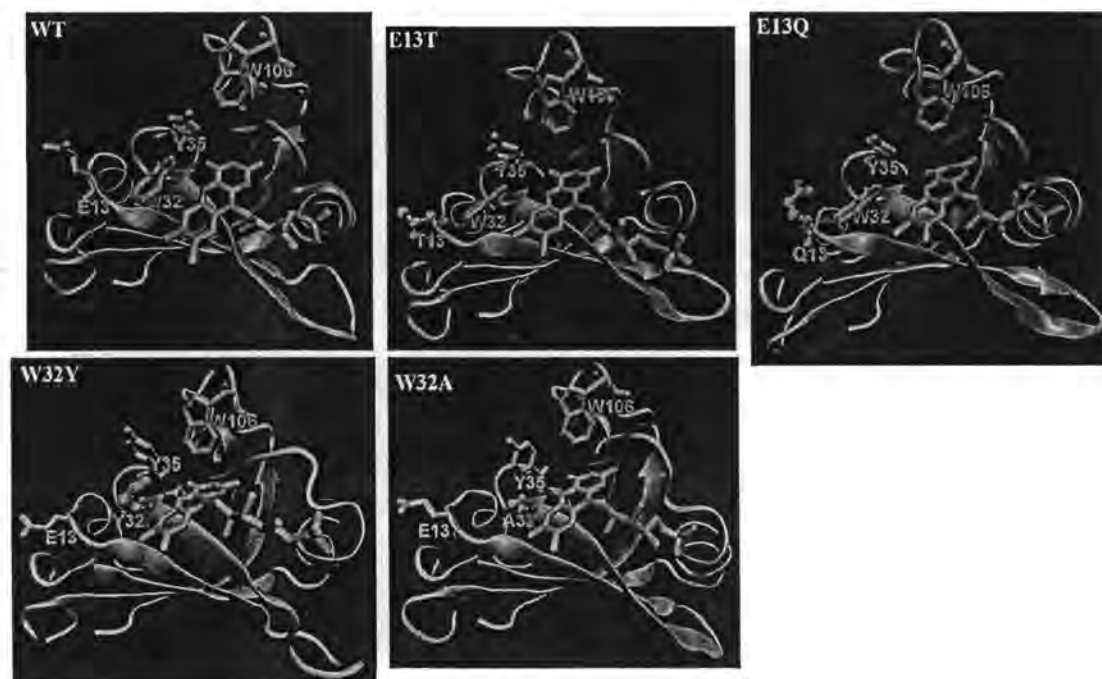


Fig. 1 Snapshots of five FBP systems (WT, E13T, E13Q, W32Y, W32A). Iso, Y35, W106 and amino acids at positions 13 and 32 are shown in stick models. WT, W32Y and W32A contain Glu13 while WT, E13T and E13Q contain Trp32, respectively.

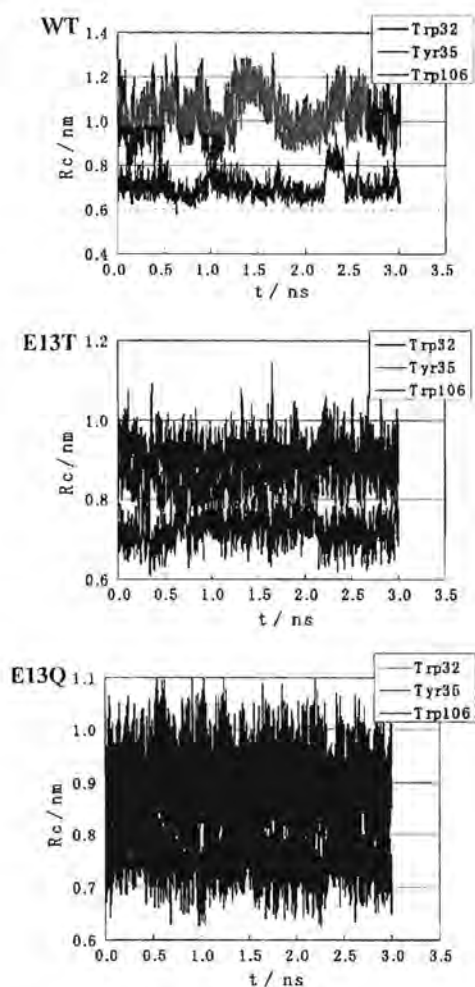


Fig. 2 Fluctuation of center-to-center distance between Iso and nearby aromatic amino acids in WT, E13T and E13Q. R_c denotes center-to-center distance. Trp32, Tyr35 and Trp106 in insets denote the R_c between Iso and these aromatic amino acids. Mean values of R_c are listed in Table 1.

the observed R_c and R_e data. The mean geometrical factors, averaged over the MD time range, are listed in Table 1. The mean R_c values between Iso and Trp32 were slightly higher in the E13T (1.03-fold) and E13Q (1.06-fold) isoforms than that for the WT, but was smaller (0.93-fold) between Iso and the Tyr32 residue in W32Y, which may be ascribed to the replacement of the Trp by the smaller Tyr residue. The R_c values between Iso and Tyr35 was shorter by 0.86-fold in E13T, by 0.84-fold in E13Q, by 0.81-fold in W32Y and by 0.76-fold in W32A, compared to the one in WT. In the W32A isoform the bulky Trp32 residue is replaced by the smaller Ala32, and so the Tyr35 might become closer to Iso. The R_c values between Iso and Trp106 were also shorter by 0.87-fold in E13T, by 0.89-fold in E13Q, by 0.86-fold in W32Y and by 0.85-fold in W32A, compared to the one in WT. These distances in the WT, E13T and E13Q isomers compare well with those obtained from the crystal structures. The R_c values between Iso and Trp32 in the crystals were 0.71 nm in all three FBP isomers, with values of 0.76–0.77 nm for the Iso-Tyr35 pair

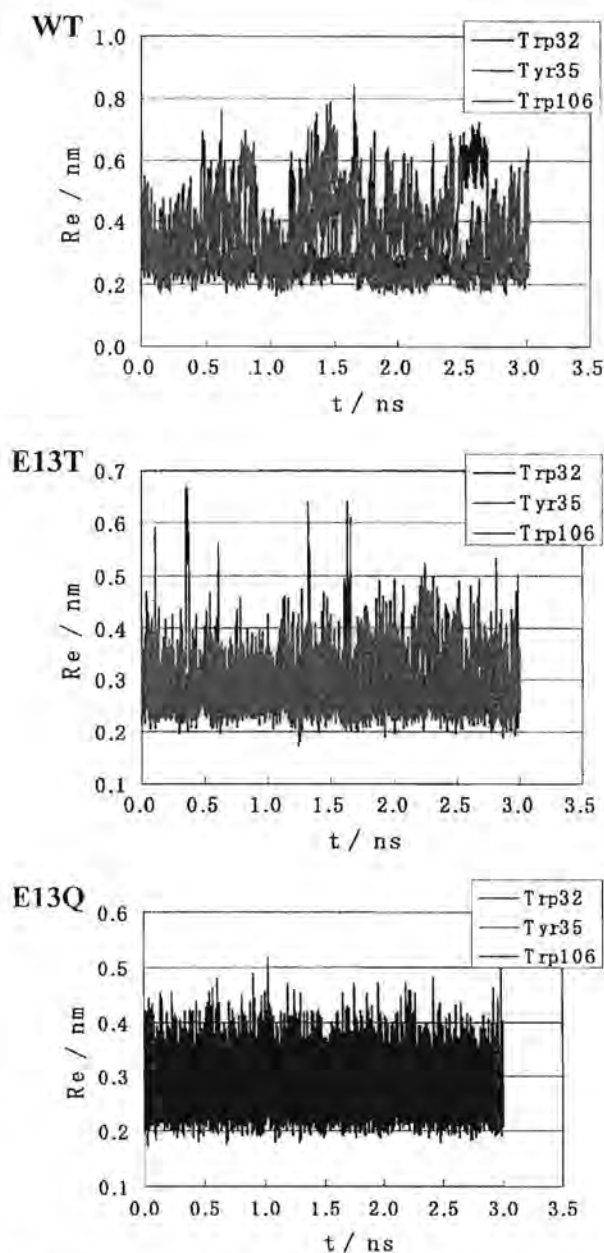


Fig. 3 Fluctuation of edge-to-edge distance between Iso and nearby aromatic amino acids. R_e denotes edge-to-edge distance. Trp32, Tyr35 and Trp106 in insets indicate R_e between Iso and these amino acids. Mean values of R_e are listed in Table 1.

and 0.84–0.85 nm for the Iso-Trp106 pair.^{27,28} In slight contrast, the R_c value for the Iso-Trp32 pair and Iso-Trp106 obtained by the MD here were 0.01–0.25 nm and 0.05–0.2 nm longer, respectively, than those obtained from the crystal structure.

The mean R_e values and the inter-planar angles between the donors and acceptor in all five FBP isoforms are also listed in Table 1. The inter-planar angles between Iso and Trp32 decreased from -52° in the WT by 9 and 14° (magnitude) in E13T and E13Q, respectively. The inter-planar angle between Iso and Tyr32 in W32Y increased by 81° compared to one in

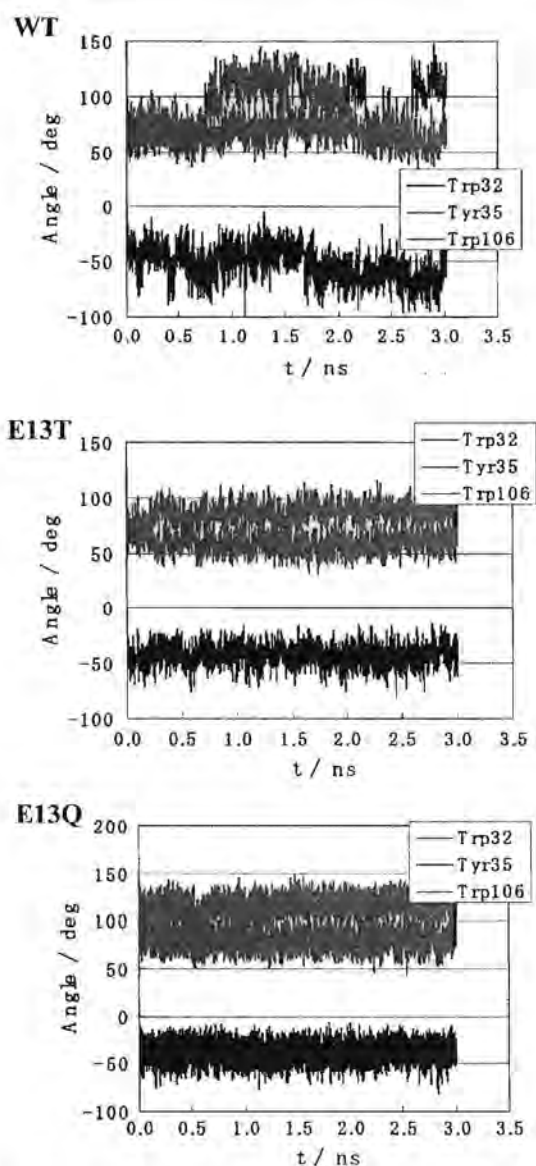


Fig. 4 Fluctuation of inter-plane angles between Iso and nearby aromatic amino acids. Trp32, Tyr35 and Trp106 in insets denote the inter-planar angles between Iso and these aromatic amino acids. Mean angles are listed in Table 1.

WT. In the W32Y isoform, Tyr32 may be quite flexible because of the smaller volume of Tyr compared to Trp. The extent of the fluctuation may be judged from the relative standard deviation (RSD) in Table 1, obtained as the SD/mean value. For all three parameters (R_c , R_e and inter-planar angle), the RSD values were highest in the WT, which implies that the WT protein structure fluctuates the most among the five FBP isoforms.

Time-dependent changes in the distances between the amino acids at position 13 and the PET donors or acceptor in all five FBP isoforms are shown in Fig. S1 (ESI† B). At a glance, the fluctuation of the distances was marked in the WT, E13Q and W32A isoforms, compared to the E13T and W32Y ones. The mean distances between these amino acid residues at the

13th position and the Iso or the PET-donor aromatic amino acid residues are listed in Table 2. The mean distances from Glu13 to Trp32 (0.92–0.98 nm) were fairly uniform across the WT, W32Y and W32A isoforms compared to that for Glu13 to Iso (1.49–1.64 nm), Tyr35 (0.99–1.46 nm) and, especially, Trp106 (1.72–2.13 nm). Indeed, the variations in the distances, as judged from the SD values, were pronounced for residue 13 to Tyr35 and Trp106, compared to those for residue 13 to Iso and Trp32.

Fluorescence dynamics

The fluorescence decays of the five FBP isoforms were simultaneously analyzed using both MH and KM theories *via* Method A. For the MH theory based analysis (Fig. 5), agreements between the observed and calculated decays were quite good in the WT, W32A and W32Y isoforms, but not so good in E13T and E13Q isoforms, especially at the long tails. For the KM theory based analysis (Fig. 6), agreements between the observed and calculated decays were quite good for the WT, E13T, E13Q and W32Y isoforms, but very poor in the W32A isoform. Thus, both the MH and KM theories did not reproduce well the single exponential decay of W32A.

The observed fluorescence decays of the WT, E13T and E13Q FBP isoforms were also analyzed with both MH and KM theories using the alternative Method B. The values of chi-square were $\chi^2_5 = 5.66 \times 10^{-3}$ by Method A and $\chi^2_3 = 9.81 \times 10^{-3}$ by Method B with MH theory, and $\chi^2_5 = 2.49 \times 10^{-3}$ by Method A and $\chi^2_3 = 1.86 \times 10^{-3}$ by Method B with KM theory. The agreements between the observed and calculated decays were better with the KM theory by both Methods A and B than with the MH theory.

PET parameters

Best-fit PET parameters with MH theory and KM theory obtained by Method A and Method B are listed in Table 3. The values of H_{Trp} were 0.015 eV by Method A, and 0.010 eV by Method B and those of H_{Tyr} were 0.00561 eV by Method A, and 0.002 eV by Method B with MH theory. These values did not differ much between the two methods. ϵ_0^{DA} is influential on ET rate through solvent reorganization energy λ_k^{R} given by eqn (2) and ES, energy between a PET donor and acceptor, $-e^2/\epsilon_0^{\text{DA}}R_{jk}$, in eqn (1) and (4). ϵ_0^{DA} was obtained as 3.33 with MH theory by Method A, and 2.36 by Method B. ϵ_0^{DA} was obtained to be 2.19 with KM theory by Method A, and 2.23 by Method B. ϵ_0^j ($j = \text{WT, E13T, E13Q, W32Y}$ and W32A with Method A, $j = \text{WT, E13T, E13Q}$ with Method B) are influential upon ET rate through $ES_j(k)$ in eqn (5) and (6). Dielectric constants determined with MH theory were $\epsilon_0^{\text{WT}} = 5.81$, $\epsilon_0^{\text{E13T}} = 5.82$, $\epsilon_0^{\text{E13Q}} = 4.83$, $\epsilon_0^{\text{W32Y}} = 13.0$ and $\epsilon_0^{\text{W32A}} = 13.0$ by Method A, and $\epsilon_0^{\text{WT}} = 8.34$, $\epsilon_0^{\text{E13T}} = 7.57$, $\epsilon_0^{\text{E13Q}} = 6.00$ by Method B. In the analysis with KM theory, PET parameters related to the electronic interaction part were taken from the previous work,²⁷ ν_0^q ($q = \text{Trp, } 1016 \text{ ps}^{-1}$; $q = \text{Tyr, } 197 \text{ ps}^{-1}$), β^q (Trp, 21.0 nm^{-1} ; Tyr, 6.25 nm^{-1}), and R_0^q (Trp, 0.663 nm ; Tyr, 0.499 nm). Dielectric constants determined with KM theory were $\epsilon_0^{\text{WT}} = 14.8$, $\epsilon_0^{\text{E13T}} = 5.99$, $\epsilon_0^{\text{E13Q}} = 6.69$, $\epsilon_0^{\text{W32Y}} = 5.89$ and $\epsilon_0^{\text{W32A}} = 6.29$ by Method A, and $\epsilon_0^{\text{WT}} = 5.82$, $\epsilon_0^{\text{E13T}} = 4.39$, and $\epsilon_0^{\text{E13Q}} = 4.82$ by Method B.

Table 1 Geometrical factors related to Iso and the indicated aromatic amino acids (PET donors) in the five FBP isomers^a

Protein system	R_c^b /nm				R_e^b /nm				Inter-planar angle/ ^o			
	Trp32	Tyr32	Tyr35	Trp106	Trp32	Tyr32	Tyr35	Trp106	Trp32	Tyr32	Tyr35	Trp106
WT	0.703	—	1.016	1.052	0.261	—	0.425	0.314	-52.2	—	93.3	67.4
(RSD ^c)	(0.072)	—	(0.097)	(0.088)	(0.086)	—	(0.292)	(0.290)	(-0.3)	—	(0.3)	(0.1)
E13T	0.724	—	0.872	0.913	0.269	—	0.331	0.269	-42.5	—	59.3	85.7
(RSD ^c)	(0.048)	—	(0.069)	(0.038)	(0.079)	—	(0.181)	(0.111)	(-0.2)	—	(0.2)	(0.1)
E13Q	0.748	—	0.854	0.939	0.265	—	0.287	0.294	-37.8	—	116.4	79.2
(RSD ^c)	(0.044)	—	(0.053)	(0.043)	(0.095)	—	(0.123)	(0.131)	(-0.2)	—	(0.1)	(0.1)
W32Y	—	0.654	0.826	0.907	—	0.276	0.284	0.251	—	28.7	76.7	77.5
(RSD ^c)	—	(0.050)	(0.075)	(0.036)	—	(0.091)	(0.167)	(0.110)	—	(0.6)	(0.1)	(0.1)
W32A	—	—	0.769	0.895	—	—	0.290	0.277	—	—	42.8	70.9
(RSD ^c)	—	—	(0.082)	(0.050)	—	—	(0.226)	(0.139)	—	—	(0.6)	(0.1)

^a Mean values of the factors between Iso and the nearby indicated aromatic amino acids are listed. The mean values were obtained by taking an average over the entire MD time range. ^b Centre-to-centre (R_c) and edge-to-edge (R_e) distances. ^c Relative standard deviation (RSD), obtained from SD/mean value.

Table 2 Mean distance between the 13th amino acid residue and the indicated aromatic amino acids (chromophores) in the five FBP isomers^a

System	Iso	Trp32	Tyr32	Tyr35	Trp106
WT ^b	1.53 ± 0.10	0.98 ± 0.09	—	0.99 ± 0.16	1.72 ± 0.15
E13T ^c	1.49 ± 0.06	0.92 ± 0.07	—	1.22 ± 0.08	1.97 ± 0.09
E13Q ^c	1.58 ± 0.13	0.98 ± 0.12	—	1.12 ± 0.16	1.84 ± 0.17
W32Y ^b	1.64 ± 0.07	—	1.13 ± 0.08	1.46 ± 0.09	2.13 ± 0.09
W32A ^b	1.60 ± 0.11	—	—	1.24 ± 0.15	1.76 ± 0.16

^a Mean distances (+1 standard deviation), averaged over the MDS time range, are shown in units of nm. ^b Distances were obtained taking the average over all distances between atoms in the aromatic ring and the center of the two oxygen atoms in the side chain of Glu13. ^c Obtained by taking the average over all distances between the atoms in the aromatic ring and the oxygen atom of the Thr13 (E13T) or Gln13 (E13Q) side chain.

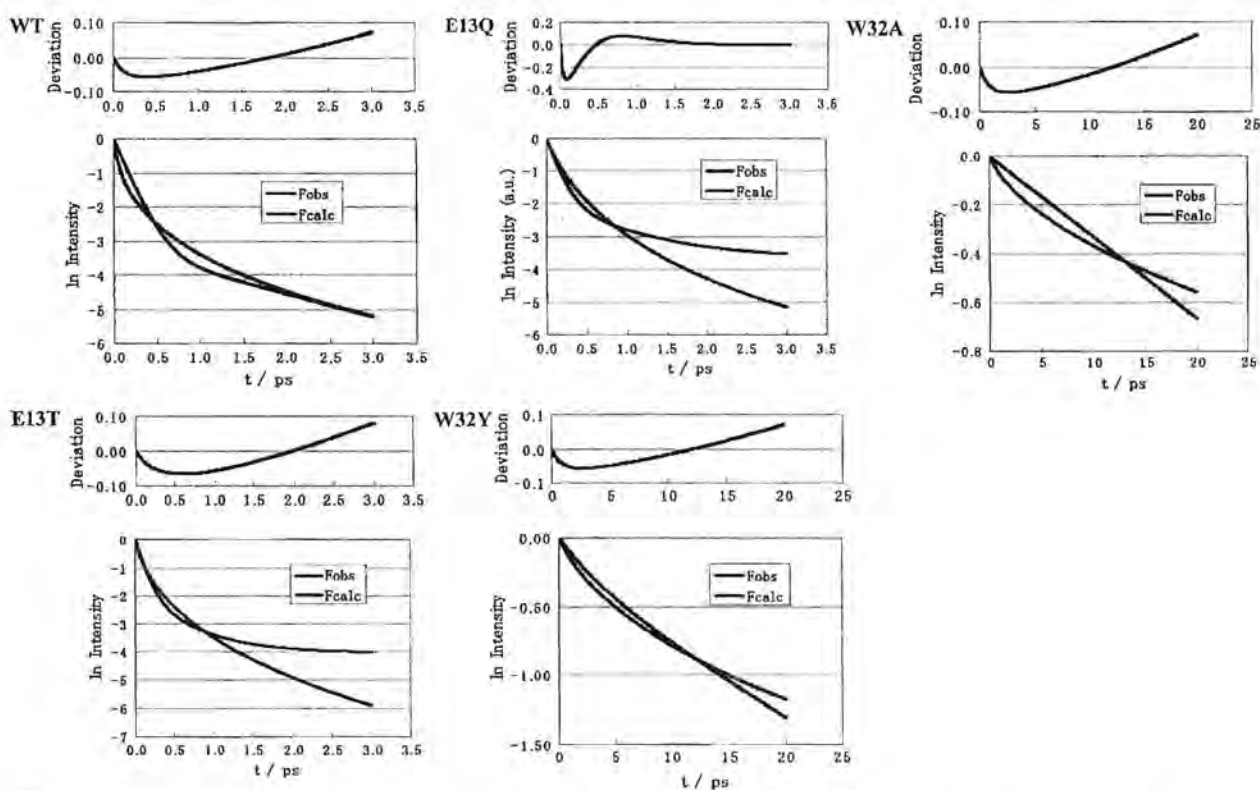


Fig. 5 Fluorescence decays of five FBP systems obtained by MH theory. F_{obs} and F_{calc} in insets denote the observed and calculated fluorescence decays. The five calculated decays were obtained with ET parameters using MH theory by Method A. Best-fit ET parameters are listed in Table 3. Upper panel of each decay represents deviation between the observed and calculated decays given by eqn (15).

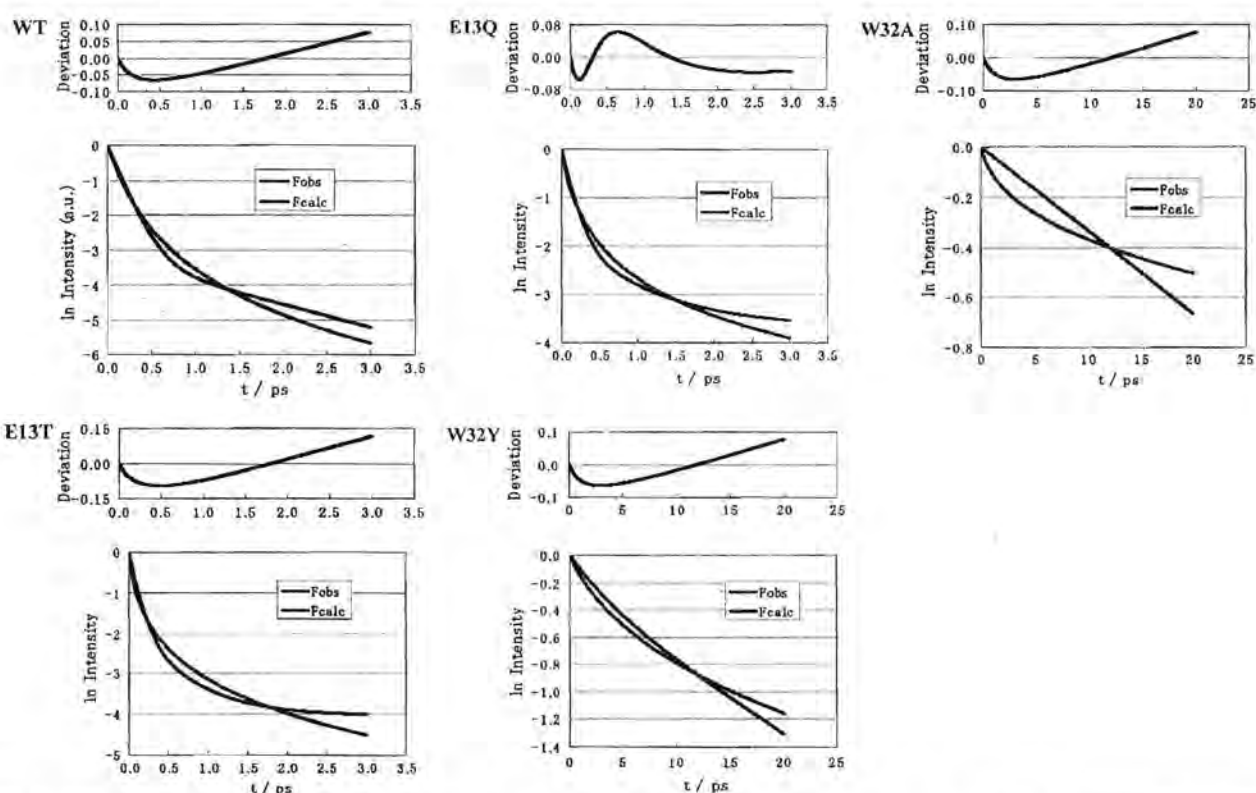


Fig. 6 Fluorescence decays of five FBP systems obtained by KM theory. F_{obs} and F_{calc} in insets denote the observed and calculated fluorescence decays. The five calculated decays were obtained with best-fit ET parameters using KM theory by Method A. The best-fit ET parameters are listed in Table 3. Upper panels of the decays represent deviations between the observed and calculated decays given by eqn (15).

Table 3 PET parameters obtained using the MH and KM theories

Theory	Method	FBP isomer					Overall					
		WT	E13T	E13Q	W32Y	W32A	ϵ_0^{DA}	G_{Iso}/eV	H_{Trp}/eV	H_{Tyr}/eV	Chi-square ^c	
MH ^a	A	ϵ_0^j	5.81	5.82	4.83	13.0	13.0	3.33	10.3	0.015	0.00561	—
		χ_j^{2h}	7.04×10^{-3}	6.59×10^{-3}	1.09×10^{-2}	1.59×10^{-3}	2.17×10^{-3}	—	—	—	—	χ_5^2 5.66×10^{-3}
KM ^e	A	ϵ_0^j	8.34	7.57	6.00	—	—	2.36	8.41	10	2.0	—
		χ_j^{2h}	1.97×10^{-2}	4.47×10^{-3}	5.30×10^{-3}	—	—	—	—	—	—	χ_5^{2d} 9.81×10^{-3}
KM ^e	B	ϵ_0^j	14.8	5.99	6.69	5.89	6.29	2.19	6.71	—	—	—
		χ_j^{2h}	1.25×10^{-3}	2.49×10^{-3}	2.09×10^{-3}	1.89×10^{-3}	4.45×10^{-3}	—	—	—	—	χ_5^2 2.49×10^{-1}
KM ^e	C ^f	ϵ_0^j	5.82	4.39	4.82	—	—	2.23	6.88	—	—	—
		χ_j^{2h}	1.19×10^{-3}	2.53×10^{-3}	1.88×10^{-3}	—	—	—	—	—	—	χ_5^2 1.86×10^{-3}
KM ^e	C ^f	ϵ_0^j	8.03	5.19	4.67	—	—	—	9.22	—	—	—
		χ_j^{2h}	—	—	—	—	—	—	—	—	—	—

^a PET rate is given by eqn (1). The meaning of the PET parameters is described below and in eqn (1). ^b χ_j^2 ($j = \text{WT, E13T, E13Q, W32Y}$ and W32A by Method A, $j = \text{WT, E13T}$ and E13Q by Method B) is defined by eqn (14). ^c χ_5^2 is defined by eqn (16). ^d χ_5^2 is defined by eqn (17). ^e The PET rate is given by eqn (4). The meaning of the PET parameters are described below eqn (4). PET parameters related to the electronic interaction part were taken from the reported values,²⁷ ν_0^q ($q = \text{Trp, } 1016 \text{ ps}^{-1}$; $q = \text{Tyr, } 197 \text{ ps}^{-1}$), β^q ($\text{Trp, } 21.0 \text{ nm}^{-1}$; $\text{Tyr, } 6.25 \text{ nm}^{-1}$) and R_0^q ($\text{Trp, } 0.663 \text{ nm}$; $\text{Tyr, } 0.499 \text{ nm}$). ^f The PET parameters are taken from a previous report determined from the crystal structures of WT, E13T and E13Q.²⁷ In this method the value of ϵ_0^{DA} was assumed to be equal to one of ϵ_0^j in respective system j ($j = \text{WT, E13T}$ and E13Q).

The dielectric constants reported with X-ray structures of WT, E13T and E13Q²⁷ were also listed in Table 3 for comparison (Method C), $\epsilon_0^{\text{WT}} = 8.03$, $\epsilon_0^{\text{E13T}} = 5.19$, and $\epsilon_0^{\text{E13Q}} = 4.67$, where KM theory was used. The values of ϵ_0^{DA} were always less than ϵ_0^j . This is reasonable because amino acid rarely exists between the donors and acceptor, while many amino acids

exist between the Iso anion or PET donor cations and ionic groups in the proteins.

The values of G_{Iso}^0 , which should be related to electron affinity of Iso*, were 10.3 eV by Method A, and 8.41 eV by Method B with MH theory. The values of G_{Iso}^0 were 6.71 eV by Method A, and 6.88 eV by Method B with KM theory.

G_{Iso}^0 may be dependent on the environment around Iso in each protein, including hydrogen bondings.

PET rate

Fig. 7 shows the time-dependent PET rates calculated using KM theory by Method A. In the WT, E13T and E13Q isoforms the PET rates were fastest from Trp32, whilst in the W32Y isoform the PET rate was fastest from Trp106, followed by Tyr32 and Tyr35. This is in agreement with previous observations that the PET rate from Tyr is always slower than that from Trp.^{23,24,27,36} The mean PET rates obtained in this study over the MD time range are listed in Table 4. The rate for Trp32 ranged from 7.1 ps^{-1} in the WT to 17.2 ps^{-1} in E13T, whilst that for Tyr32 (in W32Y) was much slower ($1.6 \times 10^{-7} \text{ ps}^{-1}$). The PET rates from Trp106 were 0.192 ps^{-1} in W32Y and 0.176 ps^{-1} in W32A.

ES energy

The time-evolution of ES energies, as expressed by eqn (5), is shown in Fig. S2 (ESI† B), where the ES energies of the Tyr35 cation were always positive. For the WT, the ES energies were

also positive for the Iso anion, but negative in the Trp106. The ES energies for Trp106 were likewise negative in the E13T and E13Q isoforms, but positive in W32Y and W32A, whilst that for Trp32 was positive in all four single substitution isoforms but fluctuating around zero in the WT. However, whilst the ES energies for Iso in W32A and W32Y were positive, as in the WT, it fluctuated around zero in both the E13T and E13Q isoforms. The difference in the ES energies between the WT and E13T or E13Q isoforms may be ascribed to the disappearance of the negatively charged Glu13 residue in the E13T and E13Q FBP isomers. Every ES energy in W32Y and W32A was always positive, and quite different from the WT, E13T and E13Q FBP isoforms.

The time-evolution of the net ES energies, as expressed by eqn (6), is shown in Fig. 8. The net ES energies of Trp32 and Tyr35 cations were always positive in all systems, whilst those for Trp106 were negative in WT, E13T and E13Q, but positive in W32Y and W32A.

Mean ES energies over MD time range are listed in Table 4. Mean ES energies of the Iso anion were 0.071 eV in WT, -0.023 eV in E13T, 0.021 eV in E13Q, 0.074 eV in W32Y and 0.079 eV in W32A. Mean ES energies of the Trp32 cation were

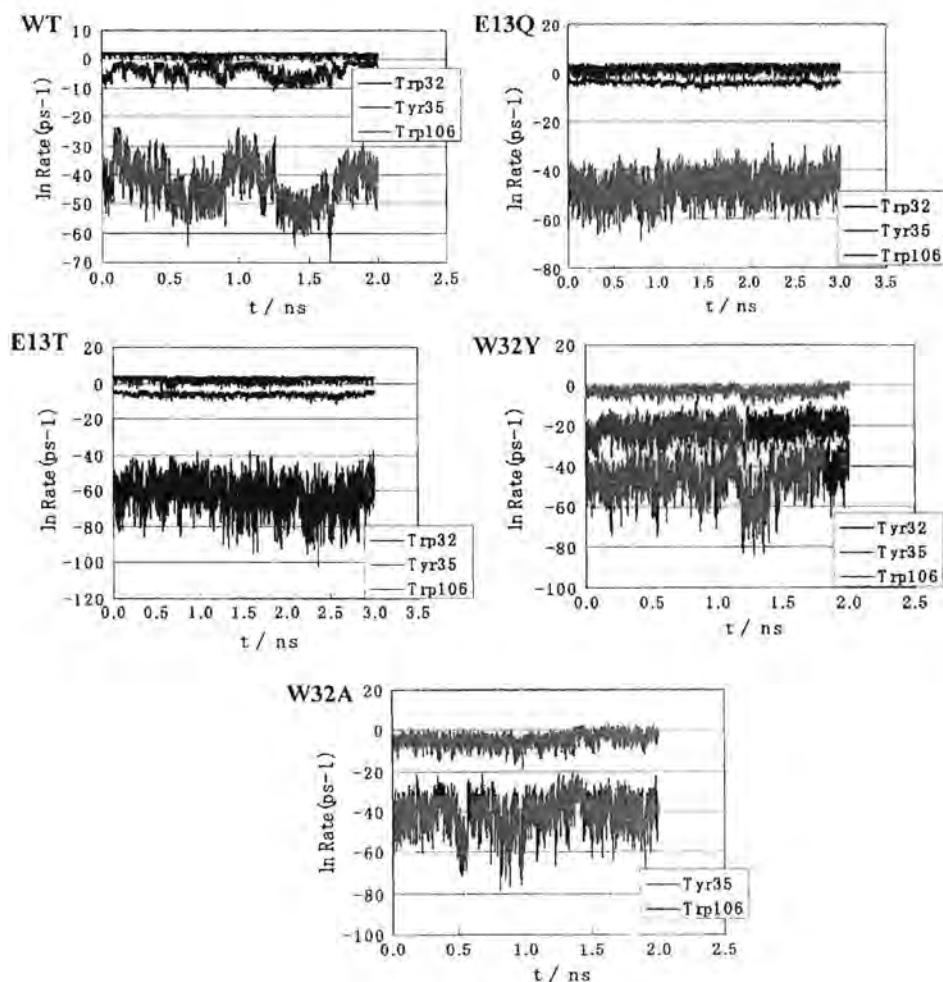


Fig. 7 ET rates from aromatic amino acids to Iso*. ET rate is expressed in units of ps^{-1} . Insets show the aromatic amino acids of ET donors. ET rates in units of ps^{-1} were obtained by ET parameters with KM theory by Method A.

Table 4 Physical quantities related to the PET rate^a

Quantity		WT	E13T	E13Q	W32Y	W32A
k_{KM}^{jk}/ps^{-1}	Trp32	7.10 ± 3.08	17.22 ± 14.76	10.81 ± 10.43	—	—
	Tyr32	—	—	—	1.6 + 30 × 10 ⁻⁷	—
	Tyr35	4 ± 95 × 10 ⁻¹⁴	6.4 ± 400 × 10 ⁻²¹	7 ± 200 × 10 ⁻¹⁷	3.7 ± 200 × 10 ⁻¹⁴	5 ± 130 × 10 ⁻¹³
	Trp106	0.082 ± 0.110	0.003 ± 0.003	0.018 ± 0.011	0.192 ± 0.350	0.176 ± 0.599
λ_S^{jk} (eV)	Trp32	0.202 ± 0.005	0.206 ± 0.004	0.208 ± 0.004	—	—
	Tyr32	—	—	—	0.217 ± 0.005	—
	Tyr35	0.249 ± 0.006	0.240 ± 0.005	0.229 ± 0.004	0.236 ± 0.006	0.231 ± 0.006
	Trp106	0.232 ± 0.005	0.223 ± 0.003	0.225 ± 0.003	0.223 ± 0.002	0.222 ± 0.003
$E_j(k)^d$ (eV)	Iso	0.071 ± 0.013	-0.023 ± 0.024	0.021 ± 0.028	0.074 ± 0.030	0.079 ± 0.026
	Trp32	0.005 ± 0.017	0.335 ± 0.043	0.269 ± 0.032	—	—
	Tyr32	—	—	—	0.123 ± 0.033	—
	Tyr35	0.080 ± 0.025	0.472 ± 0.050	0.391 ± 0.041	0.256 ± 0.052	0.242 ± 0.052
$ES_j(k)^e$ (eV)	Trp106	-0.140 ± 0.007	-0.326 ± 0.011	-0.297 ± 0.010	0.141 ± 0.039	0.230 ± 0.054
	Trp32	0.076 ± 0.010	0.312 ± 0.027	0.290 ± 0.021	—	—
	Tyr32	—	—	—	0.197 ± 0.020	—
	Tyr35	0.150 ± 0.022	0.449 ± 0.041	0.412 ± 0.035	0.330 ± 0.046	0.321 ± 0.043
$-e^2/\epsilon_0^{DA} R_{jk}^f$ (eV)	Trp106	-0.069 ± 0.017	-0.349 ± 0.025	-0.276 ± 0.029	0.215 ± 0.034	0.309 ± 0.042
	Trp32	-0.949 ± 0.055	-0.912 ± 0.045	-0.883 ± 0.045	—	—
	Tyr32	—	—	—	-1.009 ± 0.049	—
	Tyr35	-0.660 ± 0.070	-0.759 ± 0.051	-0.883 ± 0.039	-0.803 ± 0.039	-0.863 ± 0.066
$-\Delta G_T^0$ (eV)	Trp106	-0.627 ± 0.056	-0.722 ± 0.027	-0.703 ± 0.030	-0.728 ± 0.027	-0.728 ± 0.037
	Trp32	0.371	0.098	0.090	—	—
	Tyr32	—	—	—	-0.491	—
	Tyr35	-0.792	-0.992	-0.832	-0.829	-0.760
	Trp106	0.194	0.569	0.477	0.011	-0.073

^a Mean (+ 1 standard deviation) physical quantities obtained with KM theory by Method A were obtained taking an average over the entire MDS time range. ^b k_{KM}^{jk} is given by eqn (4). $j =$ WT, E13T, E13Q, W32Y and W32A. $k = 1$ for Trp32 (Tyr32 in W32Y), 2 for Tyr35 and 3 for Trp106. ^c Solvent reorganization energy given by eqn (2). The meaning of j and k are indicated in footnote b. ^d $E_j(k)$ is given by eqn (5). The meaning of j and k are indicated in footnote b. ^e Net ES energy given by eqn (6). The meanings of j and k are indicated in footnote b. ^f ES energy between a donor and acceptor. ϵ_0^{DA} is static dielectric constant in the domain between the donors and acceptor, and R_{jk} is the center-to-center distance between Iso and the indicated ET donor. The meaning of j and k is indicated in footnote b. ^g Total free energy gap, given by eqn (19).

0.005 eV in WT, 0.335 eV in E13T, 0.269 eV in E13Q. In W32Y the ES energy of the Tyr32 cation was 0.123 eV. ET rate depends on net ES energy (see eqn (1), (4) and (6)). Mean net ES energies of Trp32 were 0.076 eV in WT, 0.312 eV in E13T, 0.290 eV in E13Q. In W32Y the net ES energy of Tyr32 was 0.197 eV. Mean net ES energies of Trp106 were -0.069 eV in WT, -0.349 eV in E13T, -0.276 eV in E13Q, 0.141 eV in W32Y and 0.230 eV in W32A.

Time-dependent changes in ES energies between ET donor cations and acceptor anion are shown in Fig. S3 (ESI† B). The mean ES energies are also listed in Table 4. The energies between the Iso anion and Trp32 cation were -0.949 eV in WT, -0.912 eV in E13T, -0.883 eV in E13Q. The ES energy between the Iso anion and Tyr32 cation was -1.009 eV in W32Y. The energy of Trp32 was greatest in magnitude among three ET donors, because R_c between Trp32 and Iso was shortest.

Solvent reorganization energy

The solvent reorganization energy of the PET donor k in FBP j (λ_S^{jk}) is expressed by eqn (2), and the time-dependent changes in λ_S^{jk} are shown in Fig. S4 (ESI† B). λ_S^{jk} mostly depends on R_{jk} , because the other quantities in eqn (2) are time-independent, including ϵ_0^{DA} . The mean values of λ_S^{jk} are listed in Table 4, where for Trp32 essentially the same value (0.202–0.208 eV) was seen in the WT, E13T and E13Q isoforms, but that for Tyr32 in W32Y was slightly higher (0.217 eV). Indeed, across

all four PET donors (Trp32, Tyr32, Tyr 35 and Trp106) these values did not change much (0.2–0.25 eV).

Energy gap law. Normal energy gap law is expressed by eqn (18).

$$\ln k_{KM}^{jk} \propto (-\Delta G_T^0 + \lambda_S^{jk})^2 \quad (18)$$

Here the total free energy gap ($-\Delta G_T^0$) is given by eqn (19).

$$-\Delta G_T^0 = -\Delta G_q^0 + e^2/\epsilon_0^{DA} R_{jk} - ES_j(k) \quad (19)$$

If λ_S^{jk} varies much with the PET donor, then the following modified energy gap law may be useful.

$$(\ln k_{KM}^{jk})/\lambda_S^{jk} \propto (-\Delta G_T^0/\lambda_S^{jk} + 1)^2. \quad (20)$$

Fig. 9 shows the energy gap laws obtained with all five of the FBP isomers, with the required numerical data being summarized in Table 4. Fig. 9A shows a normal energy gap law, and Fig. 9B the modified energy gap law. In both cases, the obtained data with KM theory were expressed well by parabolic functions, being $Y = -35.24X^2 + 11.34X - 0.266$ for the normal energy gap law, where Y is $\ln k_{KM}^{jk}$ and X is $-\Delta G_T^0$, and $Y = -9.45X^2 + 8.57X + 8.89$ for the modified energy gap law, where Y is $(\ln k_{KM}^{jk})/\lambda_S^{jk}$ and X is $-\Delta G_T^0/\lambda_S^{jk}$. Variation in λ_S^{jk} was not significant because the ϵ_0^{DA} values used were common among the PET donors and FBP isoforms, and accordingly an excellent parabolic function was obtained with the normal energy gap law. The PET in these FBP isoforms mostly took

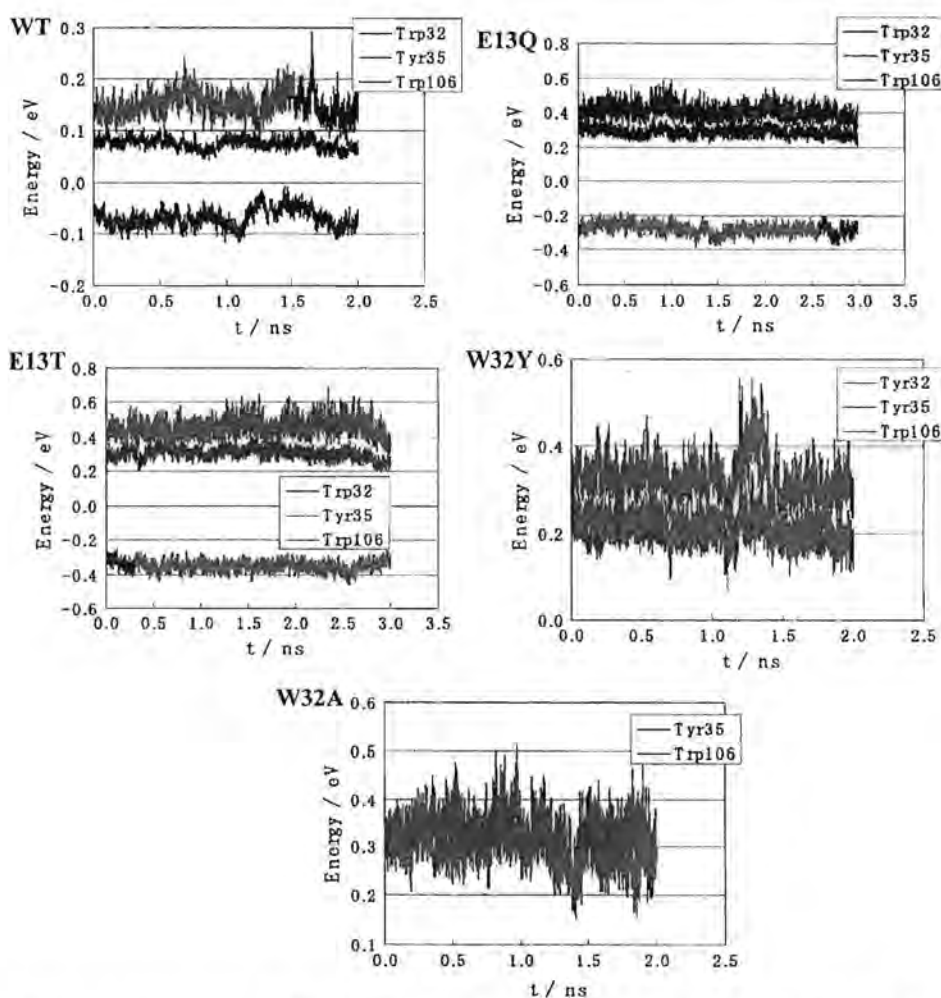


Fig. 8 Time-dependent change in net ES energy. Net ES energies (eqn (6)) were calculated with KM theory by Method A. Amino acids in insets indicate ET donors.

place in the normal region. The value of $-\Delta G_T^0$ at the maximum rate was *ca.* 0.2 eV.

IV. Discussion

In the present work the observed ultrafast fluorescence dynamics of five FBP systems were analyzed both with MH theory and KM theory based on their MD structures. The calculated decays better described the observed ones with KM theory than with MH theory, despite that both the theories are similar except for the $1 + \exp\{\beta^q(R_{jk} - R_j^0)\}$ term in KM theory (see eqn (1) and (4)). This term becomes important in a non-adiabatic ET process at $R_{jk} > R_j^0$. This may be the reason why KM theory can describe better the observed fluorescence dynamics compared to MH theory.

Here the dielectric constant of the domain between the donors and Iso (ϵ_0^{DA}) was determined separately from those of the other domains in the proteins, ϵ_0^j ($j = \text{WT, E13T, E13Q, W32Y}$ and W32A) for the first time, because amino acids rarely exist in the region between the donors and acceptor, whereas many amino acids exist in the domain between the

PET products and ionic groups in the proteins. Actually, the values of ϵ_0^{DA} were always less than those of ϵ_0^j when the analysis was performed using either MH or KM theories with either Method A or B (Table 3). The $ES_j(k)$ values were found to depend significantly on the dielectric constant (ϵ_0^j), which can vary from 1 in vacuum to 78 in water. The mean values of ϵ_0^j were 8.7, 5.9 and 5.6 in the WT, E13T and E13Q isoforms, respectively, obtained by both Methods A and B with both MH and KM theories, and 9.4 and 9.6 in the W32Y and W32A, respectively, obtained by analysis using Method A with either MH or KM theories. The dielectric constants of the WT, E13T and E13Q isoforms obtained from the X-ray structures and the average fluorescence lifetimes²⁷ (Method C in Table 3) were quite close to those obtained in the present work based upon the MD structures and the fluorescence dynamics. The dielectric constant values did not differ much among the WT (8.7), W32Y (9.4) and W32A (9.6), but those of the E13T and E13Q isoforms were 1.6-fold and 1.7-fold lower than the WT, respectively. These results are reasonable because the E13T and E13Q isoforms have one negative charge missing compared to the WT.

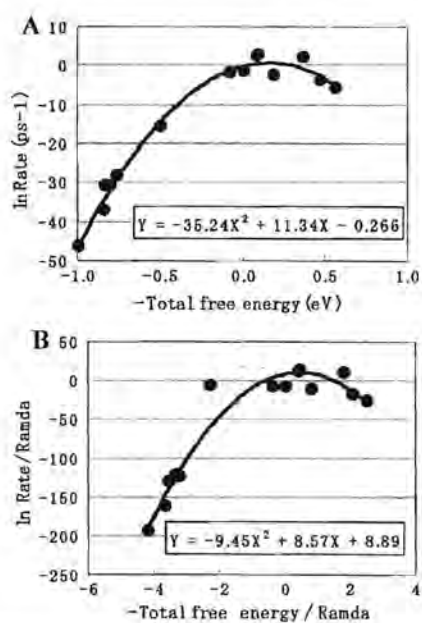


Fig. 9 Energy gap law in all FBP systems. Labels of vertical and horizontal axes indicate nk_{KM}^{jk} and $-\Delta G_T^0$ in A, and $nk_{KM}^{jk}/\lambda_S^{jk}$ and $-\Delta G_T^0/\lambda_S^{jk}$ in B, respectively. k_{KM}^{jk} is expressed in unit of ps^{-1} , and $-\Delta G_T^0$ in unit of eV. Solid lines denote approximate 2nd order polynomials, where Y and X are nk_{KM}^{jk} and $-\Delta G_T^0$ in A, and $nk_{KM}^{jk}/\lambda_S^{jk}$ and $-\Delta G_T^0/\lambda_S^{jk}$ in B, respectively.

It is important to consider which PET parameters are most influential upon the PET rate. The effect of variation in the pre-exponential factors may be not very important in terms of influencing the PET rates when determined by both MH and KM theories. Among the parameters in the exponential functions, the effect of variation in the reorganization energy (λ_S^{jk}) on the PET rates could have been suppressed because of the occurrence of λ_S^{jk} in the denominator. In the present method the values of λ_S^{jk} did not vary much between the different PET donors, because λ_S^{jk} in eqn (2) depends only on the donor-acceptor distance, R_{jk} , whereas in the former method^{25,26} λ_S^{jk} depends on both R_{jk} and dielectric constant in proteins. Actually λ_S^{jk} in Table 4 varied from 0.202 eV (Trp32 in WT) to 0.249 eV (Tyr35 in WT). It is not unreasonable to presume that the total free energy gap, as given by eqn (19), is the most influential factor upon the PET rates. $ES_j(k)$ greatly varied with the PET donor, from -0.349 eV (Trp106 in E13T; PET rate $17.22 ps^{-1}$ was fastest among the all donors) to 0.449 eV (Tyr35 in E13T; PET rate $6.4 \times 10^{-21} ps^{-1}$ was slowest), whilst those for $-\Delta G_q^0$ ($q = \text{Trp}$ or Tyr) varied at most 0.8 eV, and furthermore the ES energy between the donor and acceptor molecules ($-e^2/\epsilon_0^{DA} R_{jk}$) did from -1.009 eV (Tyr32 in W32Y) to -0.627 eV (Trp106 in WT). It may be concluded that $ES_j(k)$ is the most influential factor for PET rate in FBP systems.

According to Yoshimori *et al.*³⁷ the energy gap law becomes asymmetric along $-\Delta G_T^0$, when the effect of the electronic polarizability of solute and solvent molecules is not negligible. In the present work we have used classical KM theory in which a non-linear response due to dielectric saturation was not taken into account. Hence, the logarithm of the PET rates

obtained in this analysis could be approximated to be a parabolic function of $-\Delta G_T^0$. The energy gap law in proteins was first demonstrated in the reaction center of the purple bacterium, *Rhodobacter sphaeroides*, by Gunner and Dutton,³⁸ and the plant photosystem I and in the reaction center of the purple bacterium by Iwaki *et al.*³⁹ In these systems the PET takes place in the normal regions. Turro *et al.*⁴⁰ demonstrated that PET in a homologous series of the excited RuII diimines with cytochrome (cyt) *c* in its oxidized and reduced forms takes place in both normal region and the inverted region. In the FBP systems, the PET also took place both in the normal region and in the inverted region. At the optimal rates the free energy driving forces, $-\Delta G_T^0$, were 0.2 eV in photosystem I,³⁹ 0.7 eV in the reaction center of the purple bacterium,³⁹ the excited RuII diimine complexes—FeIIcyt *c*, 0.8 eV,⁴⁰ and the excited RuII diimine complexes—FeIIIcyt *c*, 0.9 eV.⁴⁰ In the FBP isomers it was found to be 0.2 eV (Fig. 9).

Fluctuation in the ET rates from Tyr to the excited flavin in a single molecule of flavin reductase has been observed in the time domain of sub-milliseconds to seconds.⁴¹ Fluctuation in the ET rate in the NAD(P)H : flavin oxidoreductase complex was also computationally investigated.⁴² Dutton law in which ET rate expressed as an exponentially decreasing function of the donor-acceptor distance was theoretically examined from the point of view of the donor-acceptor distance fluctuation.⁴³ In these works the fluctuation in ET rates was interpreted in terms solely of the donor-acceptor distance. Electrostatic energy in the proteins is also an important factor for the ET rate. Fluctuation in the ES energy in the proteins may also contribute to the fluctuation of the ET rate, in addition to the donor-acceptor distance.

The PET mechanism may be related in some extent to the dark electron transfer mechanism in flavoproteins. Static dielectric constant and electrostatic energies in the proteins obtained by PET analysis may be used for the electron transfer rate without light, which should also play a very important role on the dark electron transfer reactions.

Acknowledgements

The Ratchadaphiseksomphot Endowment Fund is acknowledged for financial support. The authors would like to acknowledge the Computational Chemistry Unit Cell, Chulalongkorn University and the National Center for National Nanotechnology Center (NECTEC) for the use of computing facilities. The National Center of Excellence for Petroleum, Petrochemicals, and Advanced Materials (NCE-PPAM) is also acknowledged.

References

- 1 A. M. Kuznetsov and J. Ulstrup, *Electron Transfer in Chemistry and Biology: An Introduction to the Theory*, Wiley Series in Theoretical Chemistry, John Wiley & Sons, Ltd., New York, 1999.
- 2 *Advances in Chemical Physics*, ed. J. Jortner and M. Bixon, Electron Transfer—From Isolated Molecules to Biomolecules, Wiley-Interscience, New York, 1999, vol. 106.
- 3 R. E. Blankenship, *Molecular Mechanisms of Photosynthesis*, Wiley-Blackwell, New York, 2002.
- 4 A. Möglich, X. Yang, R. A. Ayers and K. Moffat, *Annu. Rev. Plant Biol.*, 2010, **61**, 21–47.

- 5 S. Masuda and S. C. E. Bauer, *Cell*, 2002, **110**, 613–623.
- 6 Y. Shibata, Y. Murai, Y. Satoh, Y. Fukushima, K. Okajima, M. Ikeuchi and S. Itoh, *J. Phys. Chem. B*, 2009, **113**, 8192–8198.
- 7 G. Weber, *Biochem. J.*, 1950, **47**, 114–118.
- 8 D. B. McCormick, *Photochem. Photobiol.*, 1977, **26**, 169–182.
- 9 P. A. van der Berg and A. J. W. G. Visser, in *New Trends in Fluorescence Spectroscopy Applications to Chemical and Life Sciences*, ed. B. Valeur and J. C. Brochon, Springer, Berlin, 2001, pp. 457–485.
- 10 N. Mataga, H. Chosrowjan, Y. Shibata and F. Tanaka, *J. Phys. Chem. B*, 1998, **102**, 7081–7084.
- 11 N. Mataga, H. Chosrowjan, Y. Shibata, F. Tanaka, Y. Nishina and K. Shiga, *J. Phys. Chem. B*, 2000, **104**, 10667–10677.
- 12 N. Mataga, H. Chosrowjan, S. Taniguchi, F. Tanaka, N. Kido and M. Kitamura, *J. Phys. Chem. B*, 2002, **106**, 8917–8920.
- 13 F. Tanaka, H. Chosrowjan, S. Taniguchi, N. Mataga, K. Sato, Y. Nishina and K. Shiga, *J. Phys. Chem. B*, 2007, **111**, 5694–5699.
- 14 H. Chosrowjan, S. Taniguchi, N. Mataga, F. Tanaka, D. Todoroki and M. Kitamura, *J. Phys. Chem. B*, 2007, **111**, 8695–8697.
- 15 H. Chosrowjan, S. Taniguchi, N. Mataga, F. Tanaka, D. Todoroki and M. Kitamura, *Chem. Phys. Lett.*, 2008, **462**, 121–124.
- 16 A. Karen, N. Ikeda, N. Mataga and F. Tanaka, *Photochem. Photobiol.*, 1983, **37**, 495–502.
- 17 A. Karen, M. T. Sawada, F. Tanaka and N. Mataga, *Photochem. Photobiol.*, 1987, **45**, 49–54.
- 18 D. P. Zhong and A. H. Zewail, *Proc. Natl. Acad. Sci. U. S. A.*, 2001, **98**, 11867–11872.
- 19 J. Pan, M. Byrdin, C. Aubert, A. P. M. Eker, K. Brettel and M. H. Vos, *J. Phys. Chem. B*, 2004, **108**, 10160–10167.
- 20 (a) R. A. Marcus, *J. Chem. Phys.*, 1956, **24**, 966–978; (b) R. A. Marcus, *Annu. Rev. Phys. Chem.*, 1964, **15**, 155–196; (c) C. Moser, J. Keske, K. Warncke, R. Farid and P. Dutton, *Nature*, 1992, **355**, 796–801.
- 21 (a) M. Bixon and J. Jortner, *J. Phys. Chem.*, 1991, **95**, 1941–1944; (b) M. Bixon and J. Jortner, *J. Phys. Chem.*, 1993, **97**, 13061–13066; (c) M. Bixon, J. Jortner, J. Cortes, H. Heitele and M. E. Michel-Beyerle, *J. Phys. Chem.*, 1994, **98**, 7289–7299.
- 22 (a) T. Kakitani, A. Yoshimori and N. Mataga, in *Advances in Chemistry Series*, ed. J. R. Bolton, N. Mataga and G. McLendon, American Chemical Society, Washington, DC, 1991, vol. 228, pp. 45–69; (b) T. Kakitani, A. Yoshimori and N. Mataga, *J. Phys. Chem.*, 1992, **96**, 5385–5392; (c) T. Kakitani, N. Matsuda, A. Yoshimori and N. Mataga, *Prog. React. Kinet.*, 1995, **20**, 347–375.
- 23 N. Nunthaboot, F. Tanaka, S. Kokpol, H. Chosrowjan, S. Taniguchi and N. Mataga, *J. Photochem. Photobiol., A*, 2009, **201**, 191–196.
- 24 N. Nunthaboot, F. Tanaka, S. Kokpol, H. Chosrowjan, S. Taniguchi and N. Mataga, *J. Phys. Chem. B*, 2008, **112**, 13121–13127.
- 25 N. Nunthaboot, F. Tanaka and S. Kokpol, *J. Photochem. Photobiol., A*, 2009, **207**, 274–281.
- 26 N. Nunthaboot, F. Tanaka and S. Kokpol, *J. Photochem. Photobiol., A*, 2010, **209**, 70–80.
- 27 H. Chosrowjan, S. Taniguchi, N. Mataga, T. Nakanishi, Y. Haruyama, S. Sato, M. Kitamura and F. Tanaka, *J. Phys. Chem. B*, 2010, **114**, 6175–6182.
- 28 K. Suto, K. Kawagoe, N. Shibata, K. Morimoto, Y. Higuchi, M. Kitamura, T. Nakaya and N. Yasuoka, *Acta Crystallogr., Sect. D: Biol. Crystallogr.*, 2000, **56**, 368–371.
- 29 D. Case, T. Darden, T. Cheatham, C. Simmerling, J. Wang, R. Duke, R. Luo, K. Merz, B. Wang, D. Pearlman, M. Crowley, S. Brozell, V. Tsui, H. Gohlke, J. Mongan, V. Hornak, G. Cui, P. Beroza, C. Schafmeister, J. Caldwell, W. Ross and P. Kollman, *AMBER, ver. 8*, University of California, San Francisco, 2004.
- 30 J. M. Wang, P. Cieplak and P. A. Kollman, *J. Comput. Chem.*, 2000, **21**, 1049–1074.
- 31 C. Schneider and J. Suhnel, *Biopolymers*, 1999, **50**, 287–302.
- 32 U. Essmann, L. Perera, M. L. Berkowitz, T. Darden, H. Lee and G. Pedersen, *J. Chem. Phys.*, 1995, **103**, 8577–8593.
- 33 J.-P. Ryckaert, G. Cicotti and H. J. C. Berendsen, *J. Comput. Phys.*, 1977, **23**, 327–341.
- 34 V. Vorsa, T. Kono, K. F. Willey and L. Winograd, *J. Phys. Chem. B*, 1999, **103**, 7889–7895.
- 35 E. R. Henry and R. M. Hochstrasser, *Proc. Natl. Acad. Sci. U. S. A.*, 1987, **84**, 6142–6146.
- 36 N. Nunthaboot, F. Tanaka, S. Kokpol, H. Chosrowjan, S. Taniguchi and N. Mataga, *J. Phys. Chem. B*, 2008, **112**, 15837–15843.
- 37 A. Yoshimori, T. Kakitani, Y. Enomoto and N. Mataga, *J. Phys. Chem.*, 1989, **93**, 8316–8323.
- 38 M. R. Gunner and P. L. Dutton, *J. Am. Chem. Soc.*, 1989, **111**, 3400–3412.
- 39 M. Iwaki, S. Kumazaki, K. Yoshihara, T. Erabi and S. Itoh, *J. Phys. Chem.*, 1996, **100**, 10802–10809.
- 40 C. Turro, J. M. Zaleski, Y. M. Karabatsos and D. G. Nocera, *J. Am. Chem. Soc.*, 1996, **118**, 6060–6067.
- 41 H. Yang, G. Luo, P. Karnchanaphanurach, T.-M. Louie, I. Rech, S. Cova, L. Xun and X. S. Xie, *Science*, 2003, **302**, 262–266.
- 42 G. Luo, I. Andricioaei, X. S. Xie and M. Karplus, *J. Phys. Chem. B*, 2006, **110**, 9363–9367.
- 43 H. Nishioka, N. Ueda and T. Kakitani, *Biophysics*, 2008, **4**, 19–28.

Role of the Electrostatic Energy between the Photo-Products and Ionic Groups on the Photoinduced Electron Transfer from Aromatic Amino Acids to the Excited Flavins in Five FMN Binding Proteins. Effects of Negative, Positive and Neutral Amino Acids on the Rates.

Journal:	<i>The Journal of Physical Chemistry</i>
Manuscript ID:	Draft
Manuscript Type:	Article
Date Submitted by the Author:	n/a
Complete List of Authors:	Nunthaboot, Nadtanet; Mahasarakham University, Chemistry Lugsanangarm, Kiattisak; Chulalongkorn University, Chemistry Nueangaudom, Arhit; Chulalongkorn University, Chemistry Pianwanit, Somsak; Chulalongkorn University, , Chemistry Kokpol, Sirirat; Chulalongkorn University, Chemistry Tanaka, Fumio; Institute for Laser Technology, Laser Biochemistry

SCHOLARONE™
Manuscripts

1
2
3 Role of the Electrostatic Energy between the Photo-Products and Ionic Groups on the
4
5 Photoinduced Electron Transfer from Aromatic Amino Acids to the Excited Flavins in Five
6
7 FMN Binding Proteins. Effects of Negative, Positive and Neutral Amino Acids on the Rates.
8
9

10
11 Nadtanet Nunthaboot^{1*}, Kiattisak Lugsanangarm², Arthit Nueangaudom², Somsak Pianwanit²,
12
13 Sirirat Kokpol^{2,3} and Fumio Tanaka^{2,4*}
14
15

16
17 ¹ Department of Chemistry, Faculty of Science, Mahasarakham University, Mahasarakham
18
19 44150, Thailand
20

21
22 ² Department of Chemistry, Faculty of Science, Chulalongkorn University, 254 Phayathai
23
24 Road, Bangkok 10330, Thailand
25

26
27 ³ Center of Excellence for Petroleum, Petrochemicals and Advanced Materials,
28
29 Chulalongkorn University, 254 Phayathai Road, Bangkok 10330, Thailand³ Department of
30
31 Chemistry, Faculty of Science, Mahasarakham University, Mahasarakham 44150, Thailand
32

33
34 ⁴ Division of Laser Bioscience, Institute for Laser Technology, Utsubo-Honmachi, 1-8-4,
35
36 Nishiku, Osaka 550-0004, Japan
37
38
39
40
41
42
43
44
45
46
47
48
49
50
51
52
53
54
55
56
57
58
59
60

Abstract

Effects of negative, positive and neutral charges at amino acids 13 on the photoinduced electron transfer (ET) from Trp32, Tyr35 and Trp106 to the excited isoalloxazine (Iso*) have been studied in FMN binding protein (FBP) from *Desulfovibrio vulgaris* (Miyazaki F.). The protein structures of WT, E13K (Glu13 was replaced by Lys), E14R (Glu13 was replaced by Arg), E13T (Glu13 was replaced by Thr) and E13Q (Glu13 was replaced by Gln) in aqueous solution were obtained by a method of molecular dynamics simulation (MDS). The distances between the amino acids 13 and isoalloxazine (Iso), and between the amino acids and the ET donors were longer than 1 nm. The ET rates were evaluated with Kakitani and Mataga model (KM theory) from their ultrafast fluorescence dynamics by means of a non-linear least squares method. Electrostatic (ES) energies between the photo-products and other ionic groups in the proteins markedly varied among ET donors and among FBP isoforms, while the other physical quantities related to the ET rates as solvent reorganization energies and ES energies between Iso anion and the donor cations did not vary much with the proteins and with the donors. A plot of the logarithmic ET rates vs total free energy gaps displayed a parabolic function. The plot of the logarithmic rates vs the net ES energies between the photo-products and other ionic groups also displayed a parabolic function. This reveals that the net ES energies are most influential upon the ET rate, in addition to the donor-acceptor distance.

Introduction

Since a number of flavin photoreceptors have been found,¹ photochemistry and photobiology of flavoproteins have become very important field.² It is considered that the initial step of photo-regulating function by AppA is photoinduced electron transfer (ET) from Tyr to the excited isoalloxazine (Iso*) through hydrogen bonding (Hbond) chain with Gln.¹ Photochemistry of flavins has been pioneered by Weber.³ Fluorescence quenching of flavin fluorescence by indole ring was reported with isoalloxazine-(CH₂)_n-indole diads by McCormick.⁴ Time-resolved fluorescence spectroscopy of flavins and flavoproteins has been reviewed by Berg and Visser.⁵

A number of flavoproteins display practically non-fluorescent.⁶ In these flavoproteins Trp and/or Tyr always exist near isoalloxazine ring (Iso). The remarkable fluorescence quenching in these flavoproteins was demonstrated to be caused by ET from Trp and/or Tyr to the excited Iso (Iso*), by means of a picosecond⁷ and femtosecond⁸ transient absorption spectroscopy.

FMN binding protein (FBP) from *Desulfovibrio vulgaris* (Miyazaki F) is a small flavoprotein and contains flavin mononucleotide (FMN) as a cofactor, and considered to play an important role in the electron transport process in the bacterium.⁹ Three-dimensional structures of WT FBP were determined by X-ray crystallography¹⁰ and NMR spectroscopy.¹¹ According to these structures, among aromatic amino acids tryptophan 32 (Trp32) is closest to Iso, and then tyrosine 35 (Tyr35) and Trp106, respectively.

Recently, it has been demonstrated that the disappearance of only one negative charge in E13T and E13Q FBP substantially modifies the ultrafast fluorescence dynamics of wild type (WT) FBP,¹² and consequently its ET rate.¹³ It is urgent to derive more definite conclusion on a role of electrostatic (ES) energy between ionic photo-products and other ionic groups in the

1
2
3 proteins on the ET rates, since the importance of the ES energy in proteins has never been
4 recognized before.¹⁴ In the present work the effect of charge at amino acid-13 on ET rate has
5 been examined with five FBP isoforms, WT, E13K (Glu13 replaced by Lys) , E13R (Glu13
6 replaced by Arg), E13T (Glu13 replaced by Thr) and E13Q (Glu13 replaced by Gln), by
7 extracting ET rates from these ultrafast fluorescence dynamics.
8
9
10
11
12
13

14 15 **Methods of Analyses**

16 17 **Molecular Dynamic Simulation Calculation**

18
19 The structure of the WT FBP bound to FMN was retrieved from the Protein Data Bank
20 (PDB entry code 1FLM¹⁰) and was used as the starting structure for the mutated FBPs. The
21 structures of E13K and E13R FBPs were prepared in a similar fashion of E13T and E13Q in
22 the previous work.¹³ Briefly, glutamic acid at position 13 was replaced by lysine and arginine
23 for E13K and E13R, respectively. The replacement of amino acids was carried out using the
24 LEap module implemented in AMBER.¹⁵
25
26
27
28
29
30
31

32
33 All calculations were performed using AMBER 8 suite of program.¹⁵ The parm99 force
34 field¹⁶ and parameters developed by Schneider and Suhnel¹⁷ were used to treat the protein
35 and the FMN, respectively. All missing hydrogen atoms of the protein were added using
36 LEap module and the simulated systems were subsequently solvated with a cubic box of
37 6,327 TIP3P water molecules. This is almost comparable to that of 6,344 and 6,336 in the
38 case of WT, and E13Q and E13T, respectively.¹³ Two Cl⁻ counterions were added to
39 neutralize the charge of each system. The added water molecules were first minimized, while
40 protein and FMN coordinates were kept fixed. The entire system was then optimized using
41 2,000 steps of each steepest descent and conjugated gradient minimizations. Consequently,
42 the whole system was heated from 10 K to 298 K over 50 ps and was further equilibrated
43 under periodic boundary conditions at 298 K. The systems were set up under the isobaric-
44 isothermal ensemble (NPT) with a constant pressure of 1 atm and constant temperature of
45
46
47
48
49
50
51
52
53
54
55
56
57
58
59
60

298 K. Electrostatic interaction was corrected by the Particle Mesh Ewald method,¹⁸ and all bonds involving hydrogen atoms were constrained using SHAKE algorithm.¹⁹ A cutoff distance of 1 nm was employed for a non-bonded pair interaction. Molecular dynamics simulation (MDS) calculations were performed with the time steps of 2 fs and coordinates of MDS snapshot was collected every 0.1 ps. The simulations were performed over 5 ns. Data collected during the last 3 ns were used to analyze and compare with the previous MDS of WT, E13T and E13Q FBPs.¹³

ET theory. Original Marcus theory²⁰ has been modified in various ways.²¹⁻²³ In the present work KM model²³ was applied for the ET process in FBP isoforms, because it satisfactorily reproduced fluorescence decays of flavoproteins.^{13,24} The ET rate from a donor k to Iso* in the j^{th} FBP system given by KM model is expressed as eq 1.²³

$$k_{ET}^{jk} = \frac{\nu_0^q}{1 + \exp\{\beta^q(R_{jk} - R_0^q)\}} \sqrt{\frac{k_B T}{4\pi\lambda_s^{jk}}} \exp\left[-\frac{\{\Delta G_q^0 - e^2 / \epsilon_0^{DA} R_{jk} + \lambda_s^{jk} + ES_j(k)\}^2}{4\lambda_s^{jk} k_B T}\right] \quad (1)$$

Here ν_0^q is an adiabatic frequency, β^q is the ET process coefficient, and R_0^q is a critical distance between the adiabatic and non-adiabatic ET processes. It was assumed that these quantities depend only on q (Trp or Tyr), not on j and k . When $R_{jk} < R_0^q$ the ET process may be adiabatic, whereas when $R_{jk} > R_0^q$ the ET process be non-adiabatic. R_{jk} is the center to center distance between Iso and the ET donor k in the j^{th} FBP system. For this FBP, $j = 1, 2, 3, 4,$ and 5 for the WT, E13K, E13R, E13T and E13Q isoforms, respectively, while $k = 0$ for Iso, $k = 1$ for Trp32, $k = 2$ for Tyr35 and $k = 3$ for Trp106. The ET rate may be dependent on both j and k . The physical constants, \hbar , k_B , T and e are the reduced Planck's constant, Boltzmann's constant, temperature (298 K) and electron charge, respectively. ϵ_0^{DA} is a static dielectric constant of medium between ET donors and acceptor. $ES_j(k)$ is a net electrostatic (ES) energy between the k^{th} aromatic ionic species and all the other ionic groups in the j^{th}

1
2
3 FBP system, as described bellow. λ_s^{jk} is the solvent reorganization energy²⁰ of the Iso* and
4
5 the k^{th} donor in the j^{th} FBP system, as shown by eq 2.
6
7

$$\lambda_s^{jk} = e^2 \left(\frac{1}{2a_{\text{Iso}}} + \frac{1}{2a_q} - \frac{1}{R_{jk}} \right) \left(\frac{1}{\epsilon_\infty} - \frac{1}{\epsilon_0^{D\Lambda}} \right) \quad (2)$$

8
9
10 Here, a_{Iso} and a_q are the radii of Iso and the donor q (Trp or Tyr), assuming these reactants
11
12 are spherical, and ϵ_∞ is optical dielectric constant (a value of 2 being used). The radii of Iso,
13
14 Trp and Tyr were determined as previously reported,^{13,24} with values of $a_{\text{Iso}} = 0.224$ nm, and
15
16 $a_{\text{Trp}} = 0.196$ nm and $a_{\text{Tyr}} = 0.173$ nm being used.
17
18
19

20
21 The standard free energy gap (ΔG_q^0) was expressed with the ionization potential (E_{IP}^q) of
22
23 the ET donor q (Trp or Tyr), as eq 3.
24
25

$$\Delta G_q^0 = E_{\text{IP}}^q - G_{\text{Iso}}^0 \quad (3)$$

26
27 where G_{Iso}^0 is the standard Gibbs energy related to the electron affinity of Iso*. The values of
28
29 E_{IP}^q for Trp and Tyr were 7.2 eV and 8.0 eV, respectively.²⁵
30
31
32

33 ES energy in the proteins.

34
35
36 Proteins, including the FBPs, contain many ionic groups, which may influence the ET
37
38 rate. The WT, and the single-substitution E13K, E13R, E13T and E13Q isoforms, contain
39
40 Trp32, Tyr35 and Trp106 as potential ET donors. The cofactor in all these FBP systems is
41
42 FMN, which has two negative charges at the phosphate group. The WT contains 8 Glu, 5
43
44 Asp, 4 Lys and 9 Arg residues, whereas E13K contains 7 Glus, 5 Asps, 5 Lyss and 9 Args,
45
46 E13R 7 Glus, 5 Asps, 4 Lyss and 10 Args. E13T and E13Q have 7 Glus residues since the
47
48 Glu13 was replaced by the neutral Thr13 and Gln13, respectively. The ES energy between
49
50 the Iso anion or donor k -th cation, and all the other ionic groups in FBP system j is expressed
51
52 by eq 4:
53
54
55
56
57
58
59
60

$$\begin{aligned}
 E_j(k) = & \sum_{i=1}^l \frac{C_k \cdot C_{Glu}}{\epsilon_0^j R_k(Glu-i)} + \sum_{i=1}^5 \frac{C_k \cdot C_{Asp}}{\epsilon_0^j R_k(Asp-i)} \\
 & + \sum_{i=1}^m \frac{C_j \cdot C_{Lys}}{\epsilon_0^j R_k(Lys-i)} + \sum_{i=1}^n \frac{C_j \cdot C_{Arg}}{\epsilon_0^j R_k(Arg-i)} + \sum_{i=1}^2 \frac{C_j \cdot C_P}{\epsilon_0^j R_k(P-i)}
 \end{aligned} \quad (4)$$

Here $l = 8$, $m = 4$ and $n = 9$ for the WT, $l = 7$, $m = 5$ and $n = 9$ for E13K, $l = 7$, $m = 4$ and $n = 10$ for E13R, the other isoforms, and $l = 7$, $m = 4$ and $n = 9$ for E13T and E13Q. Here, $k = 0$ for the Iso anion, $k = 1$ for Trp32⁺, $k = 2$ for Tyr35⁺ and $k = 3$ for Trp106⁺. ϵ_0^j is the static dielectric constant of the j^{th} FBP system. C_k is the charge of the aromatic ionic species k , and is $-e$ for $k = 0$ (Iso anion), $+e$ for $k = 1$ to 3. C_{Glu} ($= -e$), C_{Asp} ($= -e$), C_{Lys} ($= +e$), C_{Arg} ($= +e$) and C_P ($= -e$) are the charges of Glu, Asp, Lys, Arg and phosphate anions, respectively. We assumed that these groups are all in an ionic state in solution. The values of pK_a of ionic amino acids in water were 4.3 in Glu, 3.9 in Asp, 10.5 in Lys, and 12.5 in Arg. In the proteins these values of pK_a may be modified in the range of ± 0.3 . Histidine displays 6.0 of pK_a in water. All measurements were performed in 0.1 M phosphate buffer at pH 7.0, where His should be neutral. Distances between the aromatic ionic species k and the i^{th} Glu ($i = 1 - 8$ or 7) are denoted as $R_k(Glu-i)$, those between k and the i^{th} Asp ($i = 1 - 5$) are denoted as $R_k(Asp-i)$, and so on.

$ES_j(k)$ ($k = 1 - 3$) in eqns A3 and A6 was expressed as follows:

$$ES_j(k) = E_j(0) + E_j(k) \quad (5)$$

Here, j varies from 1 to 5.

Fluorescence decays. The experimental fluorescence decay functions of the WT, E13T and E13Q, E13K and E13R FBP isoforms have been reported by Chosrowjan et al.¹² and Taniguchi et al.,²⁶ as given by eq 6. Pre-exponential factor (α_i^j) of j^{th} isoform of i^{th}

lifetime component (τ_i^j) are given in Table S1 (Supporting Information B). The lifetimes are expressed in units of ps.

$$F_{obs}^j = \sum_{i=1}^{2 \text{ or } 3} \alpha_i^j \exp(-t / \tau_i^j) \quad (6)$$

The calculated decay function of j^{th} FBP system with KM theory is expressed by eq 7:

$$F_{calc}^j(t) = \left\langle \exp \left[- \left\{ \sum_{k=1}^3 k_{KM}^k(t') \right\} t \right] \right\rangle_{AV} \quad (7)$$

The fluorescence decays of FBP isoforms were calculated up to 3 ps with 0.003 ps time intervals. Note that $\langle \dots \rangle_{AV}$ denotes the averaging procedure of the exponential function in eq 7, and was performed over t' up to ca. 3 ns with 0.1 ps time intervals. In eq 7 we assumed that the decay functions at every instant of time (t') during the MDS time range can always be expressed by an exponential function. Mathematical basis for it is described in Supporting Information A.

The unknown parameters in KM model were ν_0^q ($q = \text{Trp}$ or Tyr), β^q ($q = \text{Trp}$ or Tyr), R_0^q ($q = \text{Trp}$ or Tyr), G_{iso}^0 , ϵ_0^{WT} , ϵ_0^{E13K} , ϵ_0^{E13R} , ϵ_0^{E13T} , ϵ_0^{E13Q} and ϵ_0^{DA} . The chi-squared value of the j^{th} FBP system between the observed and calculated fluorescence intensities (χ_j^2) is defined by eq 8.

$$\chi_j^2 = \frac{1}{N} \sum_{i=1}^N \frac{\{F_{calc}^j(t_i) - F_{obs}^j(t_i)\}^2}{F_{calc}^j(t_i)} \quad (8)$$

Here, N denotes the number of time intervals of the fluorescence decay, and was 1000 for all evaluations. The deviation between the observed and calculated intensities is expressed by eq. 9.

$$Dev_j(t_i) = \frac{\{F_{calc}^j(t_i) - F_{obs}^j(t_i)\}}{\sqrt{F_{calc}^j(t_i)}} \quad (9)$$

We determined all of the unknown ET parameters, so as to obtain the minimum value of total chi-square given by eq 10, by a non-linear least square's method, according to Marquardt algorithm.

$$\chi_T^2 = \chi_{WT}^2 + \chi_{E13K}^2 + \chi_{E13R}^2 + \chi_{E13T}^2 + \chi_{E13Q}^2 \quad (10)$$

Results

Local structures of FMN binding sites. MDS snapshots near FMN binding sites of WT, E13K, E13R, E13T and E13Q are shown in Fig. 1. The FMN, Trp32, Tyr35, Trp106 and E/K/R/T/Q13 are illustrated with stick model for all isoforms. Time-evolutions of the center to center donor-acceptor distances (R_c) in E13K and E13R are shown in Figure 2. Time evolutions of R_c in WT, E13T and E13Q were reported in the previous work.¹³ Mean geometrical factors near Iso are summarized in Table 1. Data of WT, E13T and E13Q are taken from the reported work¹³ for comparison. The values of R_c between Iso and Trp32 were 0.70 nm in E13K and 0.66 nm in E13R, which are compared to those in WT, E13T and E13Q, 0.70 nm, 0.72 nm and 0.75 nm, respectively. R_c of Trp32 was shortest in E13R and longest in E13Q. The values of R_c between Iso and Tyr35 were 0.86 nm in E13K and 0.98 nm in E13R, which are compared to those in WT, E13T and E13Q, 1.02 nm, 0.87 nm, and 0.85 nm, respectively. The values of R_c between Iso and Trp106 were 0.94 nm in E13K and 0.93 nm in E13R, which did not differ much from those in E13T and E13Q, 0.91 nm and 0.94 nm, respectively. R_c of Tyr35 and Trp106 was longest in WT among five FBP isoforms.

Time-evolutions of inter-planar angles between Iso and the donors in E13K and E13R were shown in Fig. S1 in **Supporting Information B**. Mean inter-planar angles varied quite much among the five isoforms as shown in Table 1. The angles of Trp32 were -95 deg in E13K, and -78 deg in E13R. The angles of Tyr35 were 89 deg in E13K and 65 deg in E13R. The angles of Trp106 were 38 deg in E13K and 73 deg in E13R.

.1
.2
3 **Fluorescence decays.** The observed and calculated fluorescence decays of five FBP
4 isoforms are shown in Fig. 3. Agreements between the observed and calculated decay
5 functions were quite good. The values of chi-square (see Table 2) between the observed and
6 calculated decays were 1.22×10^{-3} in WT, 1.88×10^{-3} in E13K, and 1.52×10^{-3} in E13R, 2.88
7 $\times 10^{-3}$ in E13T, and 2.68×10^{-3} in E13Q. Total chi-square was 2.04×10^{-3} . The calculated
8 decays were obtained with common ET parameters, ν_0^{Trp} , ν_0^{Tyr} , β^{Trp} , β^{Tyr} , R_0^{Trp} , R_0^{Tyr} , and
9 ϵ_0^{DA} among five FBP isoforms, which are listed in Table 2. Best-fit values of ν_0^{Trp} and ν_0^{Tyr}
10 were 161 and 204 ps^{-1} , those of β^{Trp} and β^{Tyr} , 31.9 and 6.24 nm^{-1} , and those of R_0^{Trp} and
11 R_0^{Tyr} , 0.77 and 1.0 nm. The values of dielectric constant inside the proteins were $\epsilon_0^{WT}=14.2$,
12 $\epsilon_0^I = 8.08$, $\epsilon_0^U = 9.27$, $\epsilon_0^K = 11.1$, and $\epsilon_0^R = 10.2$. The dielectric constant between the donors
13 and Iso, ϵ_0^{DA} , was 2.2, which was much less than those of the entire proteins. This is
14 reasonable because no amino acid exists between Iso and the donors (Trp32, Tyr35, Trp106),
15 while many amino acids exist between the photo-products and other ionic groups.

16
17
18
19
20
21
22
23
24
25
26
27
28
29
30
31
32
33
34
35 **ET rates.** Fig. 4 shows time-evolution of logarithmic ET rate from three aromatic amino
36 acids in five FBP isoforms to Iso*. ET rates are expressed in unit of ps^{-1} . All of the
37 logarithmic ET rate markedly fluctuates with time. Fig. 5 shows distributions of logarithmic
38 ET rates in all FBP isoforms. The distribution of Trp32 displayed highly asymmetric, namely
39 sharp cut off in faster rates and long tail in slower rates. The shapes of the rate of Tyr35
40 displayed approximately symmetric along with the logarithmic rates in all FBP isoforms. The
41 shapes of Trp106 displayed a little skewed. Table 3 list ET rates evaluated by three ways,
42 Max (the logarithmic rate at maximum distribution), Av1 (integrated average over the
43 distribution) and Av2 (simple sum of the logarithmic rates divided by No. of the data). The
44 logarithmic ET rates from Trp32 displayed sharp peaks at 10.7 in WT, 14.4 in E13K, 15.3 in
45 E13R, 14.9 in E13T and 14.4 in E13Q. In E13Q the logarithmic rate showed second broad
46
47
48
49
50
51
52
53
54
55
56
57
58
59
60

1
2
3 peak at around 2, in addition to the sharp peak. The double peak shape of the distribution was
4
5 also found at -3 and -11 in Trp106 of WT.
6

7 The values of $Av1$ in Table 3 were always less than those of $Av2$. ET rate from Trp32 was
8
9 fastest among the donors. ET rate of Trp32 was fastest in E13K, then followed by E13R,
10
11 E13T, WT and E13Q. The ET rate of Trp106 was fastest in E13Q, then followed by E13T,
12
13 E13R, E13K and WT in this order.
14

15
16 **Net ES energy and ES energy between Iso anion and donor cation.** Time-evolutions of
17
18 net ES energies [$ES_j(k)$] of Trp32, Tyr35 and Trp106 given by eq 5 are shown in Fig. 6. In
19
20 Trp32 the net ES energies of WT and E13R were lowest, and highest, respectively.
21
22 Fluctuation in the net ES energy was greatest in E13R among five FBP isoforms. The
23
24 fluctuation in the net ES energy may be ascribed to the dynamics of the entire protein. In
25
26 Trp106 the net ES energy was highest in WT, which was in contract with Trp32. Distribution
27
28 of the net ES energies are shown in Fig. 7. In Trp32, the energy of WT displayed a sharp
29
30 peak at around 0.09 eV. E13R displayed double peaks, major at around 0.35 eV and minor at
31
32 around 0.24 eV. Distribution in E13K had a shoulder at right hand side. In Trp106 E13K also
33
34 displayed similar shoulder. It is evident that the net ES energy of WT was lowest in Trp32,
35
36 but highest in Trp106 among five FBP isoforms.
37
38
39
40

41 Time-evolution of ES energies between Iso anion and donor cations ($-e^2 / \epsilon_0^{DA} R_{jk}$) are
42
43 shown in Fig. 8. The fluctuation of the energies was mostly instantaneous unlike the net ES
44
45 energies, which is ascribed to local fluctuation between the donors and acceptor distances.
46
47 **Mean physical quantities related to ET rate over MDS time domain.** Table 4 lists mean
48
49 physical quantities related to ET rates in all FBP isoforms over MDS time range (ca. 30000
50
51 snapshots with 0.1 ps intervals). Solvent reorganization energy (λ_s^{jk} : see eq 2) did not vary
52
53 much among the donors and the proteins, 0.22 – 0.27 eV. This is ascribed to common
54
55
56
57
58
59
60

dielectric constant (ϵ_0^{DA}) between Iso and donors (see eq 2). Net ES energy [$ES_j(k)$] greatly varied from -0.35 eV (Trp106 in E13R) to 0.33 eV (Tyr35 in E13T). ES energy between Iso anion and a donor cation varied from -0.63 eV (Trp106 in WT) to -0.99 eV (Trp32 in E13R). The values of standard free energy gap (ΔG_q^0 ; see eq 3) were constants, 0.46 eV for Trp and 1.35 eV for Tyr as the donor.

Energy gap law. Total free energy gap was expressed by eq 11.

$$-\Delta G_T^0 = -\Delta G_q^0 + e^2 / \epsilon_0^{DA} R_{jk} - ES_j(k) \quad (11)$$

The values of $-\Delta G_T^0$ were also listed in Table 4. The values of Tyr35 were negative and markedly less than those of Trps. This may be major reason why ET rates from Tyr35 remarkably slow compared to those of Trps. The great difference in $-\Delta G_T^0$ between Tyr and Trp is ascribed to the difference in the ionization potential of Tyr (8.0 eV) and Trp (7.2 eV).²⁵ Fig. 9 shows energy gap law in five FBP isoforms. Clear parabolic function of $\ln k_{ET}^{jk}$ against $-\Delta G_T^0$ was obtained. The approximate parabolic function was expressed by a function, $Y = -44.157 X^2 + 13.337 X - 0.7391$. The maximum value of the logarithmic rate obtained by the parabolic function was 0.268 ($k_{ET}^{jk} = 1.3 \text{ ps}^{-1}$) at $-\Delta G_T^0 = 0.151 \text{ eV}$. It is noted that ET rates of Trp32 and Trp106 are mostly in so-called "inverted region".

Discussion

ET rate from individual ET donor to Iso* was extracted from ultrafast fluorescence dynamics of five FBP isoforms with negative, neutral and positive charges at amino acid-13. Distances between the amino acids-13 and Iso were around 1.5 nm. The distances between the amino acids-13 and Trp32, Tyr35, and Trp106 were around 1.0 nm, 1.2 nm and 1.8 nm, respectively. The charges at amino acid-13 quite influential upon the ET rates, though the distances from it to the ET acceptor and donors are quite far longer than 1 nm.

1
2
3 It is important to compare the ET rates obtained with crystal structures of five FBP
4 isoforms and MDS snapshots. ET rates were obtained from average lifetimes of the five FBP
5 isoforms with their crystal structures,²⁶ while the rates were obtained from fluorescence
6 decays with MDS snapshots in the present work. The ET rates from Trp32 obtained from
7 crystal structures were 4.40 ps⁻¹ in WT, 4.91 ps⁻¹ in E13K, 5.14 ps⁻¹ in E13R, 1.09 ps⁻¹ and
8 0.871 ps⁻¹ in E13Q. These values were compared with those (Av1; see Table 3) obtained by
9 MDS snapshots, were 6.11 ps⁻¹ in WT, 8.65 ps⁻¹ in E13K, 8.24 ps⁻¹ in E13R, 6.70 ps⁻¹ and
10 5.02 ps⁻¹ in E13Q. The ET rate with the crystal structures was fastest in E13R and slowest in
11 E13Q. The rate with MDS snapshots was fastest in E13K and slowest in E13Q. At any rate
12 the difference between the rates of E13K and E13R were not very much in the both methods.
13 It is noted that the ET rate was fastest in the FBP isoforms with positive charges at the amino
14 acid 13, and slowest in those with neutral charges. The ET rates obtained by MDS snapshots
15 were always faster than those with average lifetimes and crystal structures. Average lifetimes
16 depend much on the longer lifetime components, when the non-exponential decays are
17 expressed with multiple exponential functions. On the other hand the calculated decays with
18 MDS snapshots fits mostly faster component of a non-exponential decay functions. It was
19 quite difficult to reproduce the longer tail of the decay function, especially in E13T and E13Q,
20 as shown in Fig. 3. This may be the reason why the ET rates obtained with the decay
21 functions and the MDS snapshots were always faster than those obtained with the average
22 lifetimes and the crystal structures. Nevertheless the method to evaluate ET rate from a decay
23 function seems to be more useful, because MDS snapshots were obtained in water molecules,
24 while a crystal structure does not contain freely mobile water molecules, which could play
25 important role on the protein dynamics and also ET rate.

26
27
28
29
30
31
32
33
34
35
36
37
38
39
40
41
42
43
44
45
46
47
48
49
50
51
52
53
54 Effects of one amino acid charge at position 13 on the ET rates has been precisely
55 discussed with crystal structures of five FBP isoforms.²⁶ Fig. 10 shows a dependence of
56
57
58
59
60

1
2
3 logarithmic ET rates of Trp32 and Trp106 on the net ES energies [$ES_j(k)$] given by eq 5.
4
5 The net ES energy directly depends on the charge at amino acid-13. A bell shape of the
6
7 logarithmic rates vs the net ES energies was also obtained. The similarity between Fig.9 and
8
9 Fig. 10 suggests that the bell shape behavior of the logarithmic ER rate in Fig. 9 is mainly
10
11 brought about by the net ES energy, and the net ES energy is most influential factor among
12
13 energies in nuclear term of k_{ET}^{jk} .
14
15

16
17 Photoinduced and dark electron transfers in proteins have been experimentally and
18
19 theoretically investigated by many workers.^{14,21} Beratan et al.^{14c} have developed a pathway
20
21 model for electron transfer rate in proteins, based on the Fermi golden rule, in which protein
22
23 structures mediate tunnelling through bonds, through space, and through H bonds. Warshel
24
25 and Parson^{14b, 14f} formulated an electron transfer theory in proteins, while Marcus²⁰ and the
26
27 following researchers^{20, 22, 23} obtained electron transfer theories in solution. They firstly
28
29 introduced MDS to ET rate in a reaction center of bacterial photosynthetic protein from
30
31 *Rhodobacter sphaeroides*. The reaction center is complex system containing many pigments.
32
33 ET processes in flavoproteins including FBPs are much simpler than one in the reaction
34
35 center. Their theory may be tested to reproduce ultrafast fluorescence dynamics of the
36
37 flavoproteins.
38
39
40
41
42

43 44 45 46 47 48 49 50 51 52 53 54 55 56 57 58 59 60

References

- (1) (a) Crosson, S.; Moffat, K., *Proc. Natl. Acad. Sci. U.S.A.*, **2001**, *98*, 2995-3000. (b) S. Masuda, C. E. Bauer, *Cell*, **2002**, *110*, 613-623.
- (2) *Flavins: Photochemistry and Photobiology*; Silva, E.; Edwards, A. M.; Eds.; RCS Publishing, 2006.

- 1
2
3 (3) Weber, G.; *Biochem. J.*, **1950**, *47*, 114-121.
4
5 (4) McCormick, D. B.; *Photochem. Photobiol.*, **1977**, *26*, 169-182.
6
7 (5) van der Berg, P. A.; Visser, A.J.W.G. in *New Trends in Fluorescence Spectroscopy*
8 *Applications to Chemical and Life Sciences*; Valeur, B.; Brochon, J. C.; Eds., Springer, Berlin,
9 2001, pp. 457-485.
10
11 (6) (a) Mataga, N.; Chosrowjan, H.; Shibata, Y.; Tanaka, F., *J. Phys. Chem. B*, **1998**, *102*,
12 7081-7084. (b) Mataga, N.; Chosrowjan, H.; Shibata, Y.; Tanaka, F.; Nishina, Y.; Shiga, K.,
13 *J. Phys. Chem. B*, **2000**, *104*, 10667-10677. (c) Mataga, N.; Chosrowjan, H.; Taniguchi, S.;
14 Tanaka, F.; Kido, N.; Kitamura, M., *J. Phys. Chem. B*, **2002**, *106*, 8917-8920. (d) Tanaka, F.;
15 Chosrowjan, H.; Taniguchi, S.; Mataga, N.; Sato, K.; Nishina, Y.; Shiga, K., *J. Phys. Chem.*
16 *B*, **2007**, *111*, 5694-5699. (e) Chosrowjan, H.; Taniguchi, S.; Mataga, N.; Tanaka, F.;
17 Todoroki, D.; Kitamura, M., *J. Phys. Chem. B*, **2007**, *111*, 8695-8697. (f) Chosrowjan, H.;
18 Taniguchi, S.; Mataga, N.; Tanaka, F.; Todoroki, D.; Kitamura, M., *Chem. Phys. Lett.*, **2008**,
19 *462*, 121-124.
20
21 (7) (a) Karen, A.; Ikeda, N.; Mataga, N.; Tanaka, F., *Photochem. Photobiol.*, **1983**, *37*, 495-
22 302. (b) Karen, A.; Sawada, M. T.; Tanaka, F.; Mataga, N., *Photochem. Photobiol.*, **1987**, *45*,
23 49-53.
24
25 (8) Zhong, D. P.; Zewail, A. H., *Proc. Natl. Acad. Sci. U. S. A.*, **2001**, *98*, 11867-11872.
26
27 (9) Kitamura, M.; Kojima, S.; Ogasawara, K.; Nakaya, T.; Sagara, T.; Niki, K.; Miura, H.;
28 Akutsu, K.; Kumagai, I., *J. Biol. Chem.* **1994**, *269*, 5566-5573.
29
30 (10) Suto, K.; Kawagoe, K.; Shibata, N.; Morimoto, K.; Higuchi, Y.; Kitamura, M.; Nakaya,
31 T.; Yasuoka, N., *Acta Crystallogr., Sect. D*, **2000**, *56*, 368-371.
32
33 (11) Liepinsh, L.; Kitamura, M.; Murakami, T.; Nakaya, T.; Otting, G., *Nat. Struct. Biol.*
34 **1997**, *4*, 975-979.
35
36
37
38
39
40
41
42
43
44
45
46
47
48
49
50
51
52
53
54
55
56
57
58
59
60

- 1
2
3 (12) Chosrowjan, H.; Taniguchi, S.; Mataga, N.; Nakanishi, T.; Haruyama, Y.; Sato, S.;
4
5 Kitamura, M.; Tanaka, F., *J. Phys. Chem. B*, **2010**, *114*, 6175-6182.
6
7 (13) Nunthaboot, N.; Pianwanit, S.; Kokpol, S.; Tanaka, F., *Phys. Chem. Chem. Phys.*, **2011**,
8
9 *13*, 6085-6097.
10
11 (14) (a) Warshel, A.; Chu, Z. T.; Parson, W.W., *Science*, **1989**, *246*, 112-116, (b) Warshel,
12
13 A.; Parson, W.W., *Rev. Phys. Chem.* **1991**, *42*, 279-309, (c) Beratan, D. N.; Betts, J. N.;
14
15 Ounchic, J. N., *Science*, **1991**, *252*, 1285-1288, (d) Bendall, D. S. *Protein Electron Transfer*.
16
17 BIOS Scientific Publishers Ltd., Oxford, UK, 1996, (e) Gray, H. B.; Winkler, J. R., *Annu.*
18
19 *Rev. Biochem.*, **1996**, *65*, 537-561, (f) Warshel, A.; Parson, W.W., *Quart. Rev. Biophys.* **2001**,
20
21 *34*, 563-679.
22
23 (15) Case, D.; Darden, T.; Cheatham, T.; Simmerling, C.; Wang, J.; Duke, R.; Luo, R.; Merz,
24
25 K.; Wang, B.; Pearlman, D.; Crowley, M.; Brozell, S.; Tsui, V.; Gohlke, H.; Mongan, J.;
26
27 Hornak, V.; Cui, G.; Beroza, P.; Schafmeister, C.; Caldwell, J.; Ross W.; Kollman, P.,
28
29 AMBER, ver. 8, University of California, San Francisco, 2004.
30
31 (16) Wang, J. M.; Cieplak, P.; Kollman, P. A., *J. Comput. Chem.*, **2000**, *21*, 1049-1074.
32
33 (17) Schneider, C.; Suhnel, J., *Biopolymers*, **1999**, *50*, 287-302.
34
35 (18) Essmann, U.; Perera, L.; Berkowitz, M. L.; Darden, T.; Lee, H.; Pedersen, *J. Chem.*
36
37 *Phys.*, **1995**, *103*, 8577-8593.
38
39 (19) Ryckaert, J.-P.; Cicotti, G.; Berendsen, H. J. C., *J. Comput. Phys.*, **1977**, *23*, 327-341.
40
41 (20) (a) Marcus, R. A.; *J. Chem. Phys.*, **1956**, *24*, 966-978. (b) Marcus, R. A., *J. Chem.*
42
43 *Phys.* **1956**, *24*, 979-989. (c) Marcus, R. A., *Annu. Rev. Phys. Chem.*, **1964**, *15*, 155-196.
44
45 (21) Moser, C.; Keske, J. M.; Warncke, K.; Farid, R. S.; Dutton, P. L., *Nature*, **1992**, *355*,
46
47 796-802.
48
49
50
51
52
53
54
55
56
57
58
59
60

- 1
2
3 (22) (a) Bixon, M.; Jortner, J., *J. Phys. Chem.*, **1991**, *95*, 1941-1944, (b) Bixon, M.; Jortner, J.,
4 *J. Phys. Chem.*, **1993**, *97*, 13061-13066, (c) Bixon, M.; Jortner, J.; Cortes, J.; Heitele, H.;
5 Michel-Beyerle, M. E., *J. Phys. Chem.*, **1994**, *98*, 7289-7299.
6
7
8
9 (23) (a) Kakitani, T.; Mataga, N., *J. Phys. Chem.* **1985**, *89*, 8-10., (b) Kakitani, T.; Yoshimori,
10 A.; Mataga, N., in *Advances in Chemistry Series*; Bolton, J. R.; Mataga, N.; McLendon, G.,
11 Eds., American Chemical Society, Washington, DC, **1991**, vol. 228, pp. 45-69. ; (c) Kakitani,
12 T.; Yoshimori, A.; Mataga, N., *J. Phys. Chem.*, **1992**, *96*, 5385-5392.
13
14 (24) (a) Nunthaboot, N.; Tanaka, F.; Kokpol, S.; Chosrowjan, H.; Taniguchi, S.; Mataga, N.,
15 *J. Photochem. Photobiol. A*, **2009**, *201*, 191-196, (b) Nunthaboot, N.; Tanaka, F.; Kokpol, S.;
16 Chosrowjan, H.; Taniguchi, S.; Mataga, N., *J. Phys. Chem. B*, **2008**, *112*, 13121-13127. (c)
17 Lugsanangarm, K.; Pianwanit, S.; Kokpol, S.; Tanaka, F.; Chosrowjan, H.; Taniguchi, S.;
18 Mataga, N., *J. Photochem. Photobiol. A*, **2011**, *219*, 32-41.
19
20 (25) Vorsa, V.; Kono, T.; Willey, K. F.; Winograd, L., *J. Phys. Chem. B*, **1999**, *103*, 7889-
21 7895.
22
23 (26) Taniguchi, S.; Chosrowjan, H.; Tanaka, F.; Nakanishi, T.; Sato, S.; Haruyama, Y.;
24 Kitamura, M., submitted.
25
26
27
28
29
30
31
32
33
34
35
36
37
38
39
40
41
42
43
44
45
46
47
48
49
50
51
52
53
54
55
56
57
58
59
60

Table 1 Geometrical factors related to Iso and the indicated aromatic amino acids in the five FBP isomers.^a

Protein system	Rc ^b / nm			Re ^c / nm			Inter-planar angle ^d / deg		
	Trp32	Tyr35	Trp106	Trp32	Tyr35	Trp106	Trp32	Tyr35	Trp106
WT ^e	0.703	1.016	1.052	0.261	0.425	0.314	-52	93	67
E13K	0.701	0.857	0.936	0.278	0.283	0.250	-95	89	38
E13R	0.664	0.977	0.933	0.259	0.322	0.237	-78	65	73
E13T ^e	0.724	0.872	0.913	0.269	0.331	0.269	-43	59	86
E13Q ^e	0.748	0.854	0.939	0.265	0.287	0.294	-38	116	79

^aMean values of the factors between Iso and the nearby indicated aromatic amino acids are listed. The mean values were obtained by taking an average over the entire MD time range.

^bCentre-to-centre distance.

^cEdge-to-edge (Re) distances.

^dInter-panar angle between Iso and indicated aromatic amino acid.

^eData taken from Ref 13.

Table 2 Best-fit ET parameter^a

ν_0^{Tnp} (ps ⁻¹)	ν_0^{Tyr} (ps ⁻¹)	β^{Tnp} (nm ⁻¹)	β^{Tyr} (nm ⁻¹)	R_0^{Tnp} (nm)	R_0^{Tyr} (nm)
161	204	31.9	6.24	0.770	1.00
ϵ_0^{WT}	ϵ_0^K	ϵ_0^R	ϵ_0^T	ϵ_0^Q	ϵ_0^{DA}
14.2	11.1	10.2	8.08	9.27	2.20
χ_{WT}^2	χ_K^2	χ_R^2	χ_T^2	χ_Q^2	χ_{Total}^2
1.22×10^{-3}	1.88×10^{-3}	1.52×10^{-3}	2.88×10^{-3}	2.68×10^{-3}	2.04×10^{-3}

^a Indexes WT, K, R, T, and Q for the static dielectric constant ϵ_0 and chi-square χ^2 denote

WT, E13K, E13R, E13T and E13Q FBPs, respectively. The values of G_{iso}^0 was 6.65 eV.

Table 3 ET rate^a

Donor		WT	E13K	E13R	E13T	E13Q
Trp32	Max ^b	10.7	14.4	15.3	14.9	14.4
	Av1 ^c	6.11	8.65	8.25	6.70	5.02
	Av2 ^d	7.02	10.2	9.75	8.27	6.57
Tyr35	Max ^b	1.12×10^{-18}	3.68×10^{-17}	1.64×10^{-22}	3.12×10^{-22}	6.78×10^{-17}
	Av1 ^c	9.17×10^{-20}	9.19×10^{-18}	1.48×10^{-23}	6.99×10^{-23}	2.87×10^{-17}
	Av2 ^d	1.21×10^{-14}	2.12×10^{-13}	1.05×10^{-20}	3.50×10^{-17}	1.53×10^{-14}
Trp106	Max ^b	2.50×10^{-2}	6.74×10^{-3}	4.17×10^{-3}	4.37×10^{-2}	5.13×10^{-2}
	Av1 ^c	9.89×10^{-4}	4.53×10^{-3}	4.57×10^{-3}	3.31×10^{-2}	3.80×10^{-2}
	Av2 ^d	2.08×10^{-2}	6.71×10^{-3}	6.19×10^{-3}	3.93×10^{-2}	5.54×10^{-2}

a ET rates were evaluated in the three ways, and expressed in unit of ps⁻¹.

b ET rates at maximum distributions.

c Average rates were evaluated by integrations over logarithmic rate distributions.

d Average rates were evaluated by simple sums divided by number of logarithmic rates

1
2
3
4
5
6
7
8
9
10
11
12
13
14
15
16
17
18
19
20
21
22
23
24
25
26
27
28
29
30
31
32
33
34
35
36
37
38
39
40
41
42
43
44
45
46
47
48
49
50
51
52
53
54
55
56
57
58
59
60

Table 4 Physical quantity related to ET rate^a

Protein	Donor or acceptor	$E_j(k)^b$ (eV)	$\lambda_s^{jk\ c}$ (eV)	$ES_j(k)^d$ (eV)	$-e^2 / \epsilon_0^{DA} R_{jk}^e$ (eV)	ΔG_g^{0f} (eV)	$-\Delta G_T^{0g}$ (eV)	$\ln k_{ET}^{jk\ h}$
WT	Iso	0.067						
	Trp32	0.00907	0.220	0.0759	-0.935	0.548	0.311	1.81
	Tyr35	0.0863	0.270	0.153	-0.650	1.35	-0.851	-43.8
	Trp106	-0.138	0.250	-0.0717	-0.627	0.548	0.150	-6.92
E13K	Iso	-0.0848						
	Trp32	0.283	0.219	0.198	-0.937	0.548	0.191	2.16
	Tyr35	0.292	0.259	0.207	-0.767	1.35	-0.787	-39.2
	Trp106	-0.263	0.243	-0.348	-0.700	0.548	0.500	-5.40
E13R	Iso	-0.0676						
	Trp32	0.376	0.214	0.309	-0.987	0.548	0.130	2.11
	Tyr35	0.344	0.268	0.276	-0.671	1.35	-0.953	-52.6
	Trp106	-0.282	0.243	-0.350	-0.702	0.548	0.504	-5.39

1									
2									
3									
4									
5	E13T	Iso	-0.0187						
6									
7		Trp32	0.242	0.223	0.224	-0.905	0.548	0.134	1.90
8									
9		Tyr35	0.352	0.260	0.334	-0.754	1.35	-0.928	-51.0
10									
11		Trp106	-0.240	0.241	-0.258	-0.717	0.548	0.427	-3.41
12									
13									
14	E13Q	Iso	0.0141						
15									
16		Trp32	0.193	0.225	0.207	-0.876	0.548	0.121	1.61
17									
18		Tyr35	0.279	0.248	0.293	-0.876	1.35	-0.765	-38.1
19									
20		Trp106	-0.215	0.243	-0.201	-0.698	0.548	0.351	-3.27
21									
22									

a Mean values over MD time range.

b ES energy given by eq 4

c Solvent reorganization energy given by eq 2.

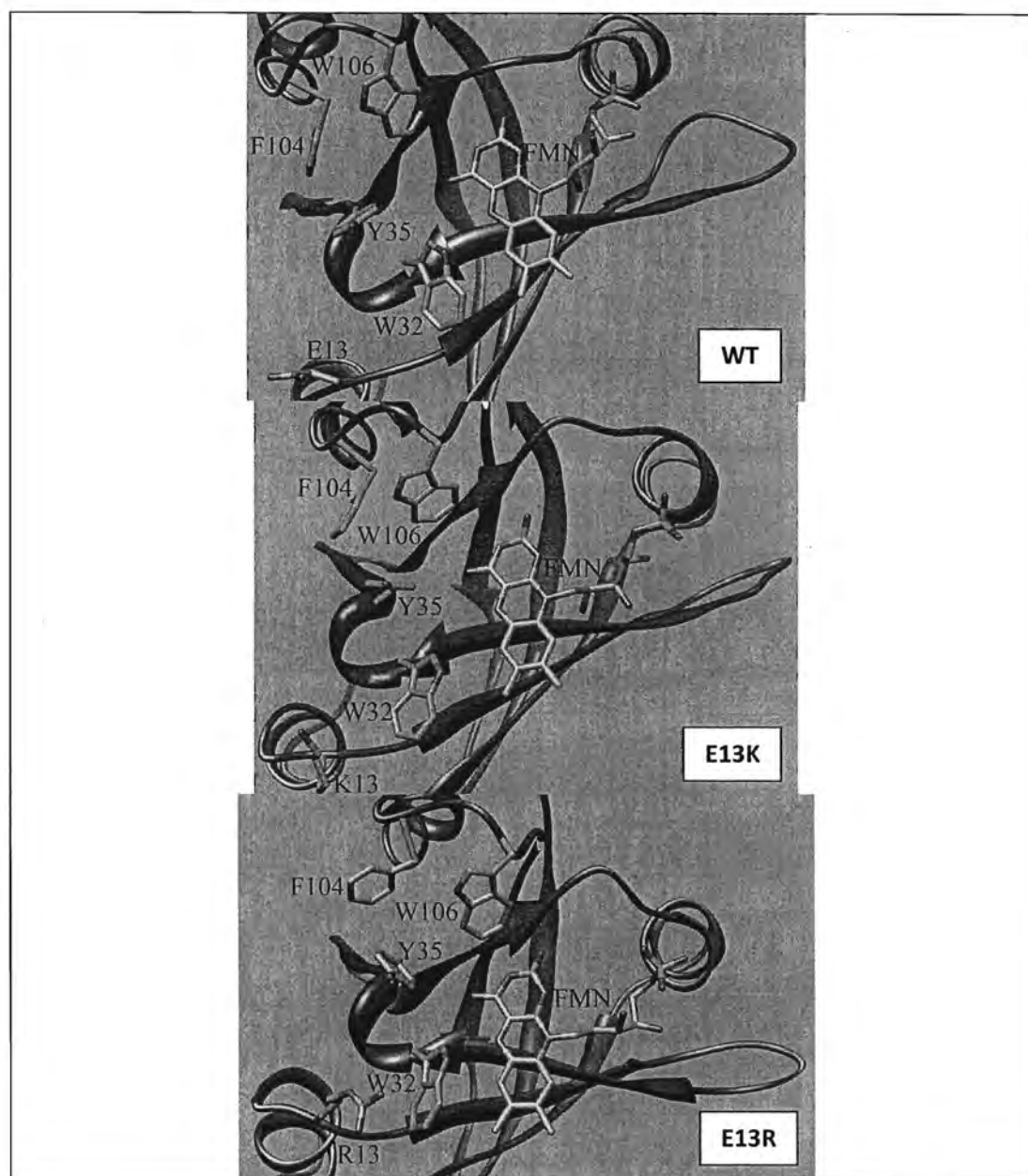
d Net ES energy given by eq 5.

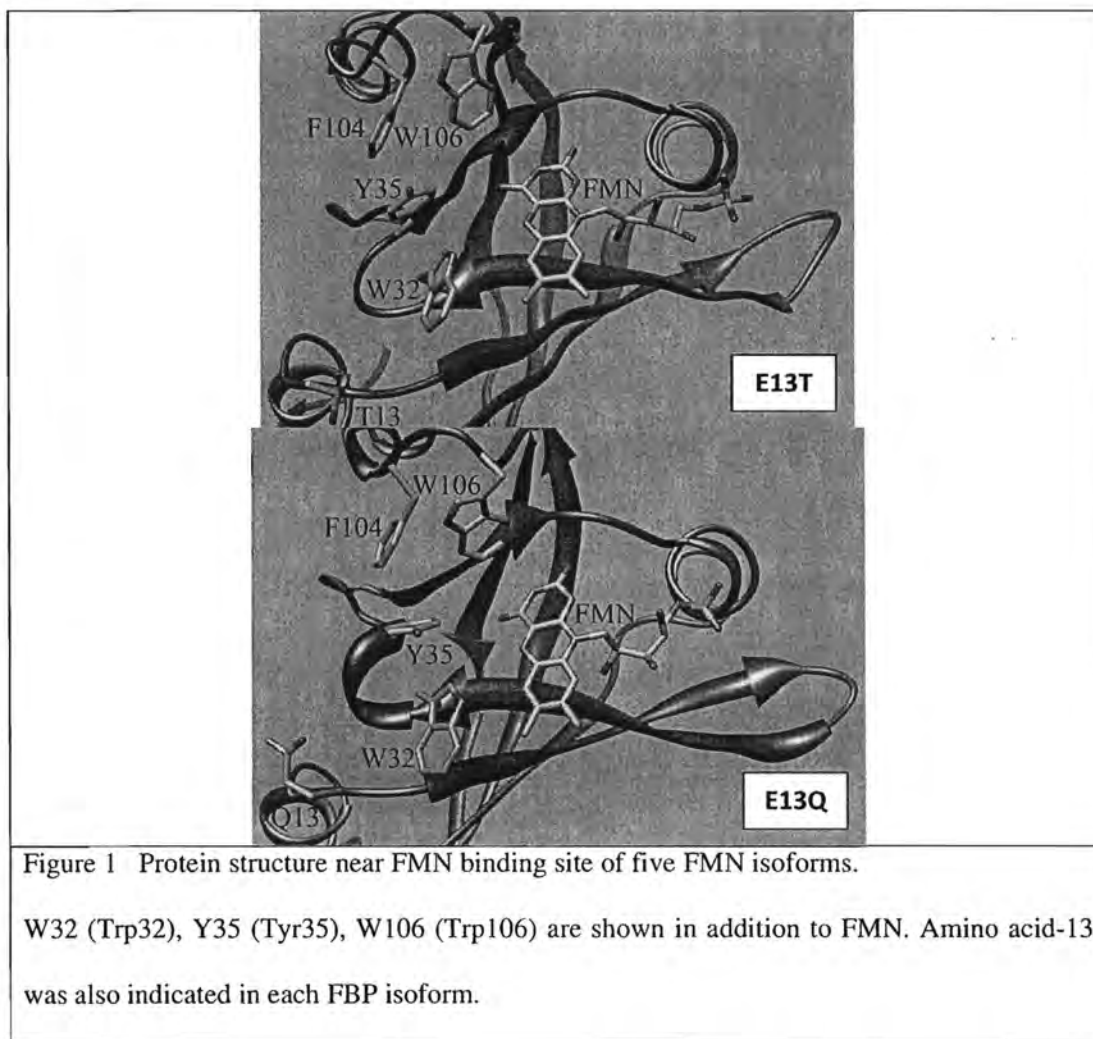
e ES energy between Iso anion and Trp or Tyr cation.

f Standard free energy gap given by eq 3.

g Total free energy gap given by eq 17.

h logarithmic ET rate evaluated by integrated average (see Table 3).





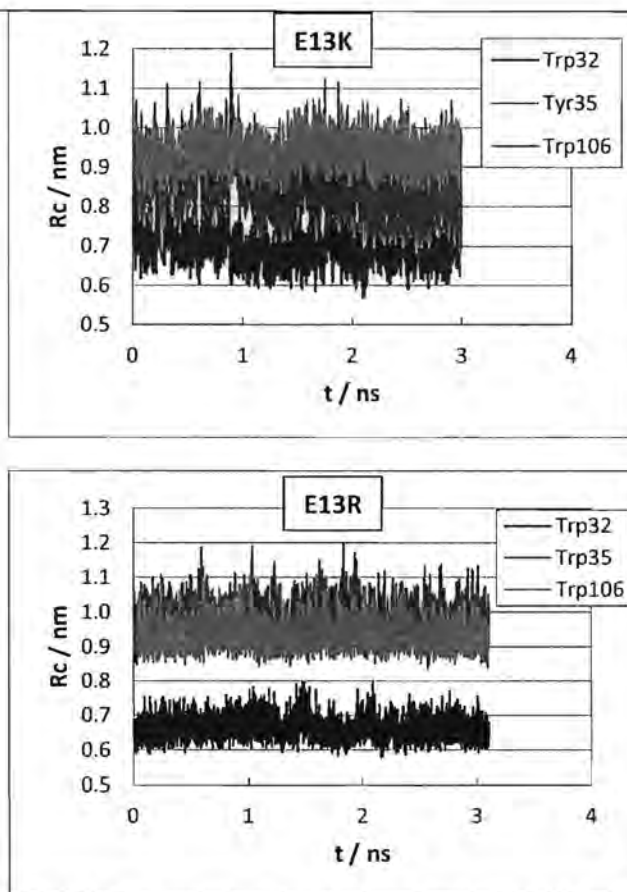
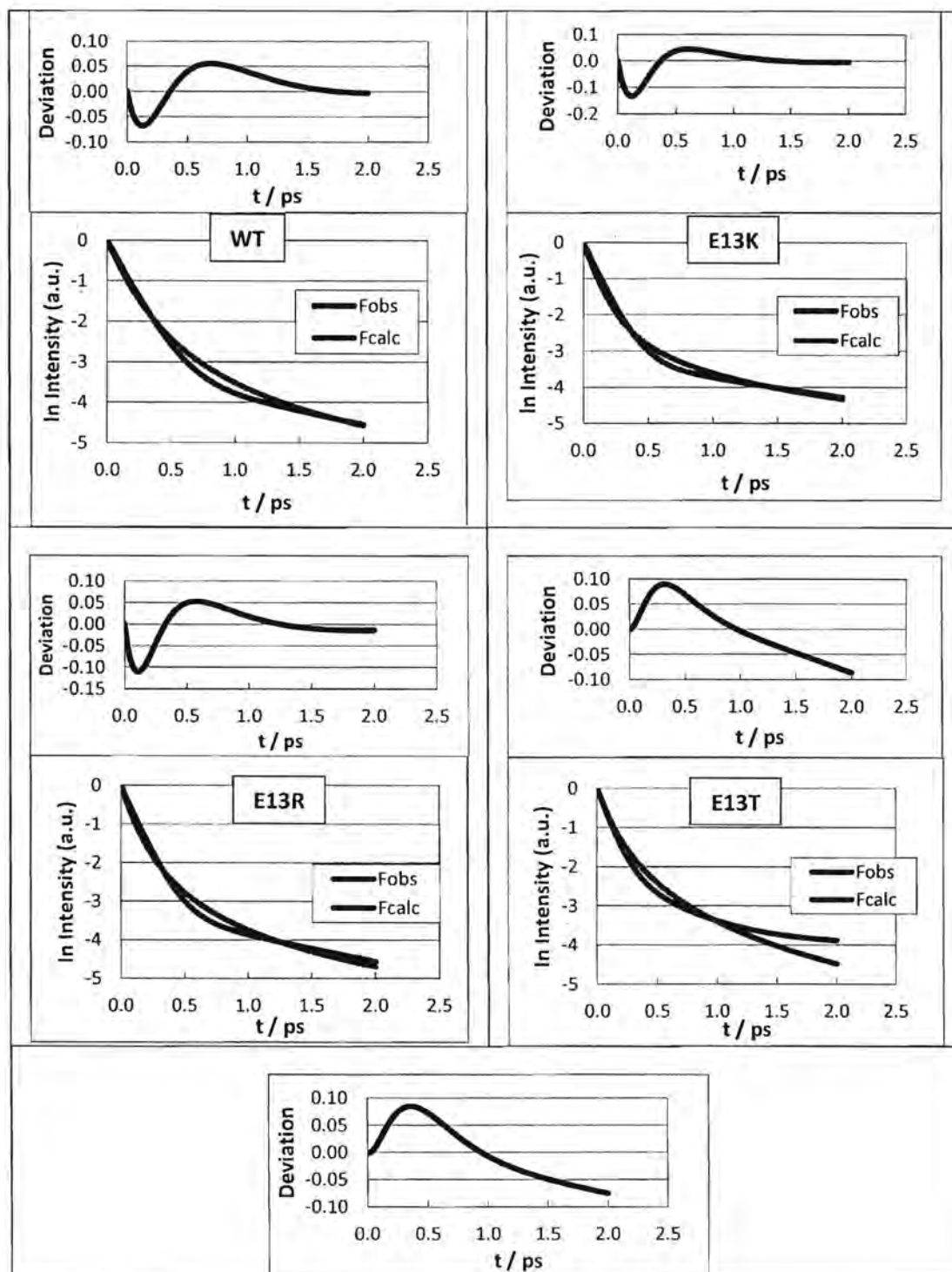
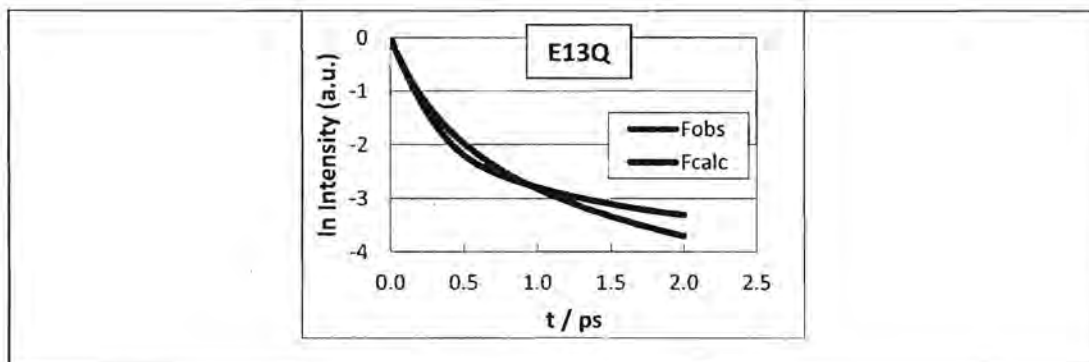


Figure 2 Dynamics of the ET donor-acceptor distance in E13K and E13R

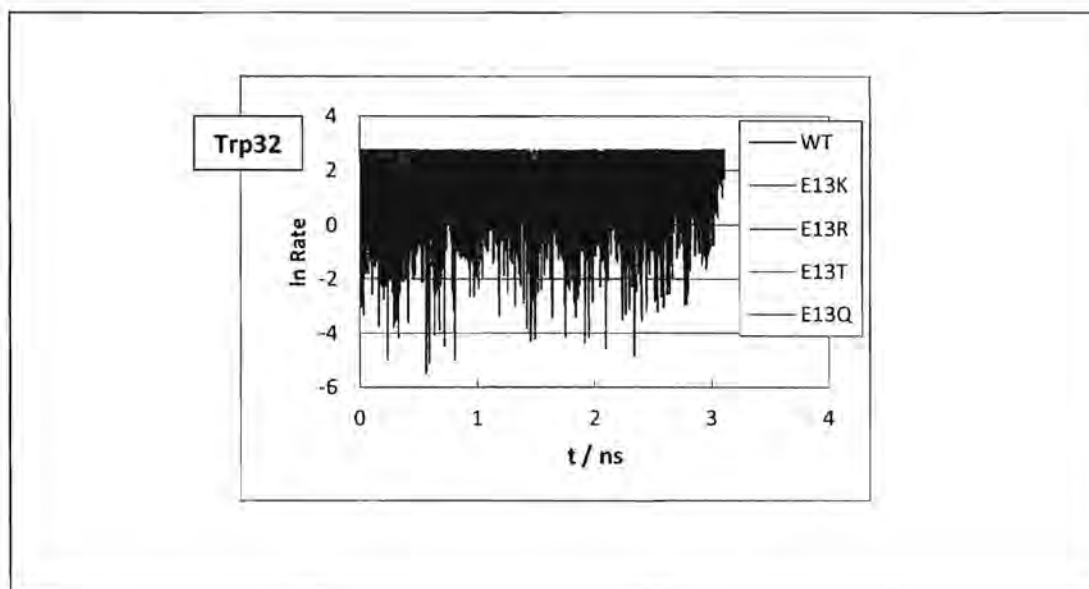
Center to center distance (R_c) between Iso and ET donors indicated in inserts.





15
16
17
18
19
20
21
22
23
24
25
26

Figure 3 The observed and calculated fluorescence decays of five FBP isoforms. The calculated fluorescence decays (Fcalc) were obtained by the method described at **Methods of Analyses**.



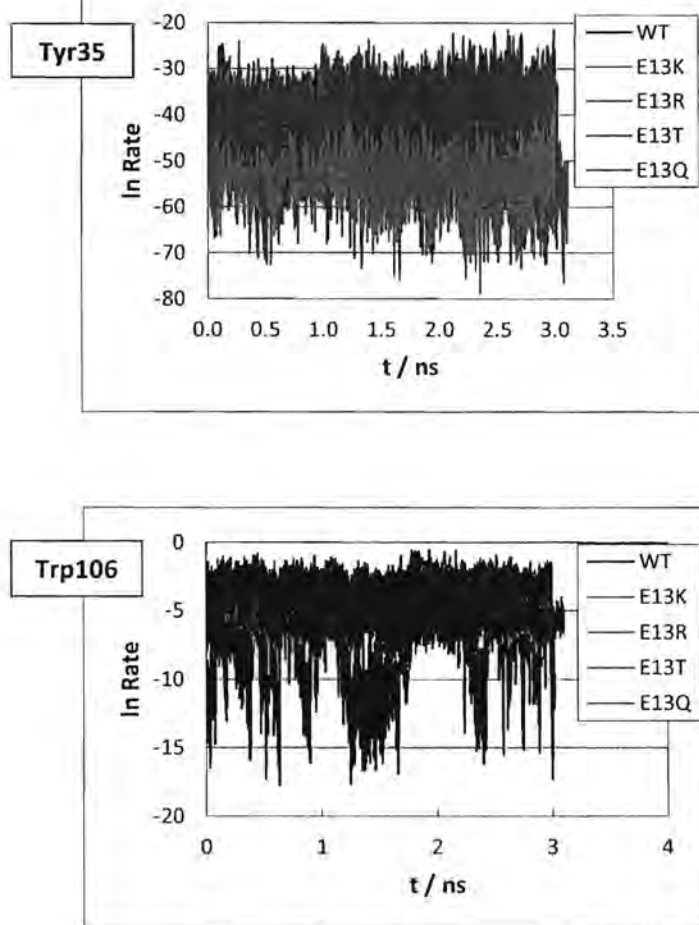
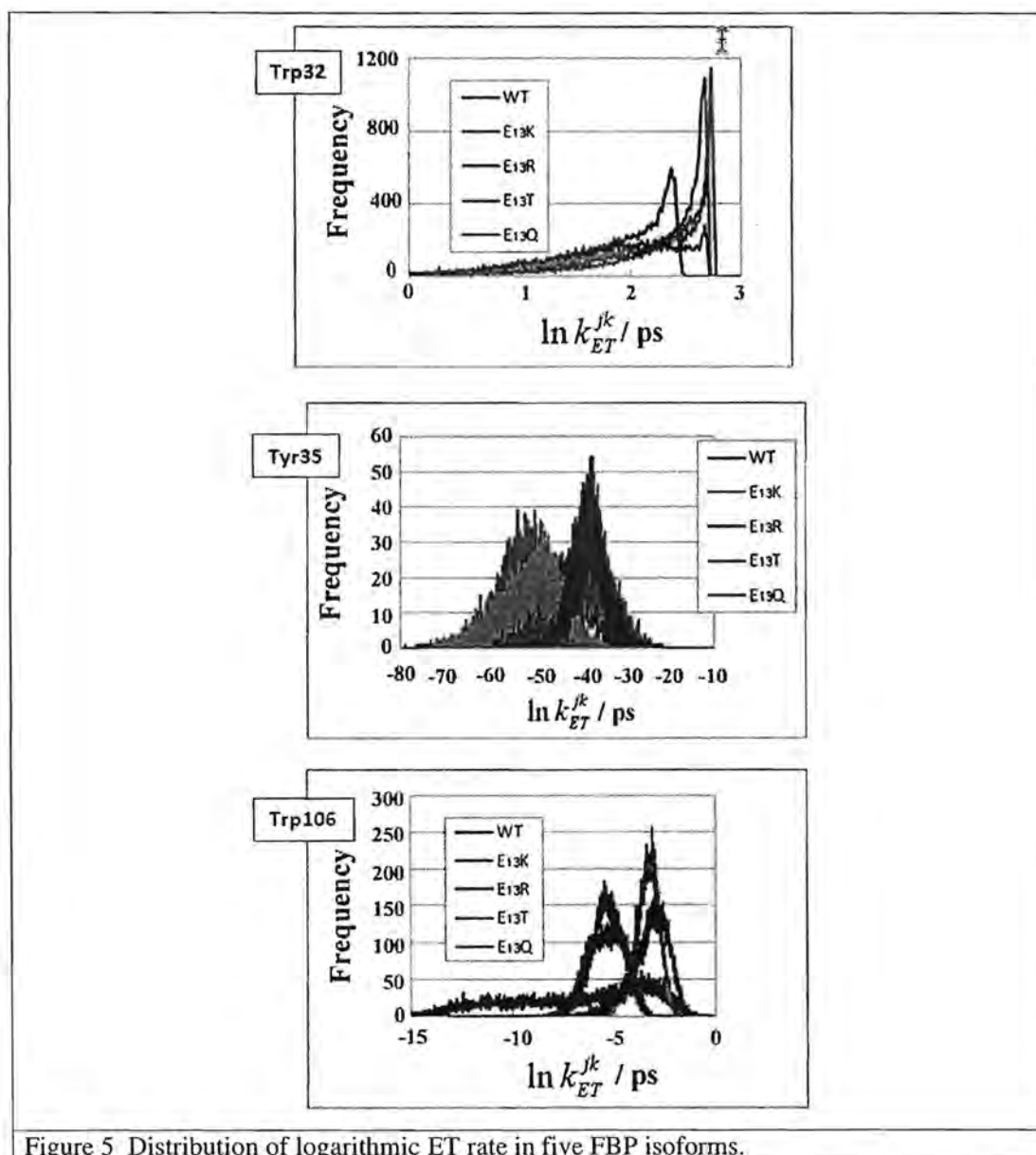


Figure 4 Time-evolution of ET rates from aromatic amino acids to Iso*

ET rates are expressed in ps^{-1} unit. Inserts indicate FBP isoforms.



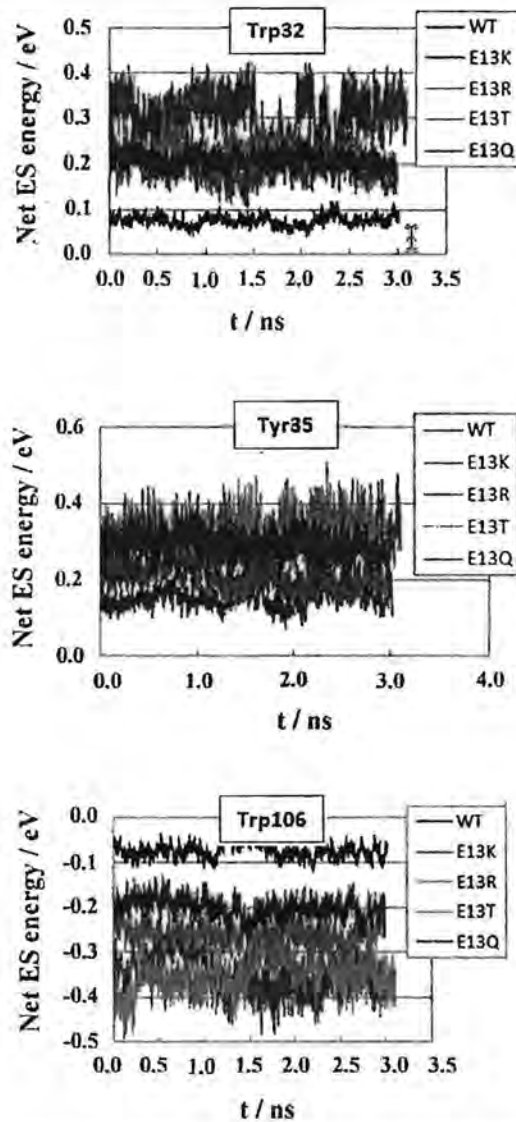


Figure 6 The time-evolution of Net-ES energies of potential ET donors in five FBP isoforms.

Net ES energy, $ES_j(k)$, were obtained by eqs 4 and 5.

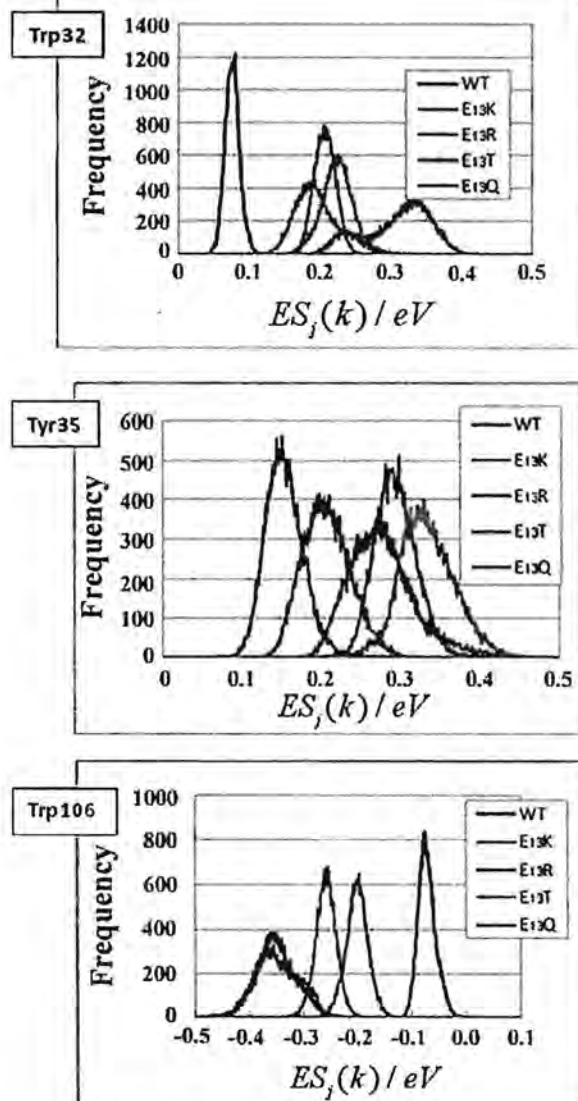


Figure 7 Distribution of Net ES energy.

Net ES energy, $ES_j(k)$, is given by eqs 4 and 5.

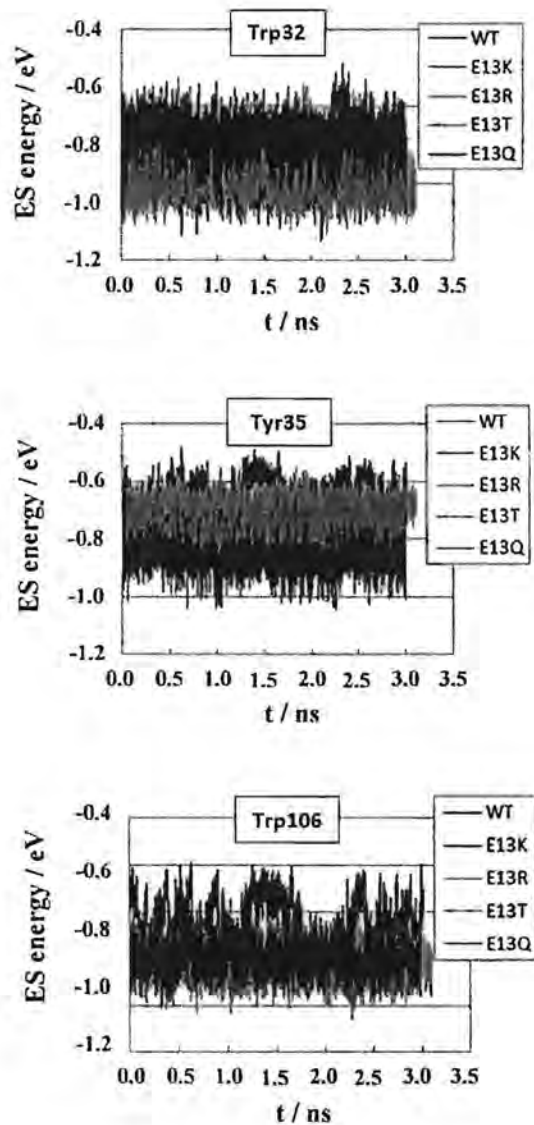


Figure 8 ES energy between the donor and acceptor.

ES energies between Iso anion and the donor cations. Inserts indicate five FBP isoforms.

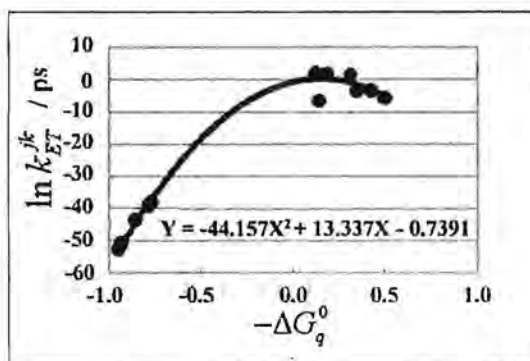


Figure 9 Energy gap law of Trp32 and Trp106 as the ET donors in five FBP systems.

Total free energy gap, $-\Delta G_T^0$ in eV unit, was obtained by eq 11. Insert indicates approximate parabola function of logarithmic ET rate (Y) vs $-\Delta G_T^0$ (X).

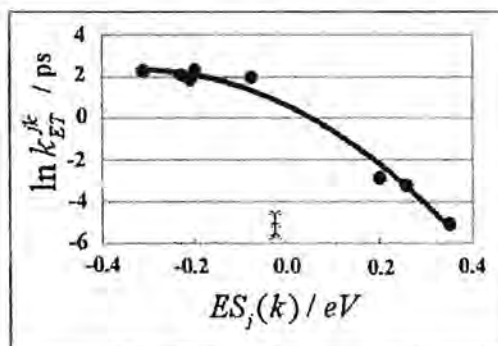


Figure 10 Dependence of logarithmic ET rate of Trp on Net ES energy.

The logarithmic ET rates of Trp32 and Trp106 were plotted against net ES energies. Sign of net ES energies were changed to see the similarity with the energy gap law shown in Fig. 9.

1
2
3
4
5
6
7
8
9
10
11
12
13
14
15
16
17
18
19
20
21
22
23
24
25
26
27
28
29
30
31
32
33
34
35
36
37
38
39
40
41
42
43
44
45
46
47
48
49
50
51
52
53
54
55
56
57
58
59
60